DANYUO YIPORO (ID No: 40178)

IMPLANTABLE BIOMEMS DEVICES FOR LOCALIZED BREAST CANCER DRUG-DELIVERY

A THESIS

SUBMITTED TO THE GRADUATE FACULTY

IN PARTIAL FULFILLMENT OF THE REQUIREMENT FOR THE

DEGREE OF

MASTER OF SCIENCE

DEPARTMENT OF MATERIALS SCIENCE AND ENGINEERING

SUPERVISOR: PROF. WINSTON WOLE SOBOYEJO

ADVISER: DR. ODUSANYA SHOLA

DECEMBER, 2011

DEDICATION

I dedicate this thesis to the entire Ottour's family, my parents, Mr. Danyuo, Mrs. Tumbo Danyuo, my grandmother, Mrs. Nirkwieriyir Dar, my brothers and sisters, and my loving wife, Mrs. Mary Yiporo, and most especially to you, my son, Kenneth N. Yiporo, with love.

ABSTRACT

Implantable Bio-Micro-Electro-Mechanical Systems (BioMEMS) represent a new class of devices that can provide localized cancer drug delivery by the combined effect of chemotherapy and hyperthermia which gives it an advantage over prior devices. The current work presents the results of a theoretical and experimental study of a novel implantable drug delivery device. Prototype Poly-di-methyl-siloxane (PDMS) packages with well-controlled micro-channels, and a drug storage compartments were fabricated along with a drug storing polymer produced by free radical polymerization of Poly(N-isopropylacrylamide)(PNIPA), comonomers of Acrylamide (AM). The swelling due to the uptake of water, bromophenol blue and a bacterial extract prodigiosin (an apoptotic agent), were studied using weight gain experiments conducted over temperatures within the range in which hyperthermia (28-48^{o}C) could occur during drug delivery. These studies provided understanding of the underlying mechanisms of diffusion and swelling of these PNIPA-based gels. The results show that drug release may be well described by monolithic and membrane diffusion models. The in-vitro studies at 43˚C indicate that a lesser amount of drug delivery is achieved when the delivery is accompanied with heat. Morphological studies with an environmental Scanning Electron Microscope (SEM) reveal a polymeric network of the PNIPA-based gels. The diffusion coefficients obtained varied from 2.10 x10^{-12} m^2/s at 28˚C to 4.8162x10^{-6} m^2/s at 48˚C. The results obtained from the released exponent as well as the diffusion coefficient from the gels were consistent to prior work [1- 3]. Prior work [2] indicated diffusion coefficients of PNIPA which were found to be within 0.2 x 10^{-12} m^2/s and 4 x 10^{-12} m^2/s, which was said to be dependent on the network densities of the gels. Recent work [1] also revealed diffusion coefficient for PNIPA within 1.68x10^{-12} m^2/s at 37˚C to 1.12x10^{-6} m^2/s at 45˚C. The release exponents indicated a domination of non-Fickian diffusion.

Contents Pages

List of Figures

LIST OF TABLES

Acknowledgments

My soul shall praise the living God. He alone answered my prayers. I am glad with what God has done for me in my life, most especially seeing me through my MSc program in African University of Science and Technology. I cannot imagine how success could come my way if my God was not by my side.

My heart is filed with joy and I am glad to have a supervisor like Prof. Winston Wole Soboyejo. With all his busy schedules, he made it possible for me to get all that is required to make this a reality.

My sincere gratitude goes to my advisor, Dr. Odusanya Shola for his assistance in the lab; Shedah Science and Technology Complex, Abuja.

Moreover, I am grateful to the financiers through World Bank Step B, which took all upon itself to finance the project geared toward targeting and treating cancer.

I must thank all those who worked with me on this project, specifically, Ilouno Mercy Chikaodili, Meshack Taahyam Maureen, Ani N. Joy, Oberaifo Omoyeme Ejeme, Ani Nwanake Joy S.O. Dozie-Nwachukwu, G.A. Etuk-Udo, and Debora O.

My gratitude further goes to my friends, students, staff and professors, here at African University of Science and Technology. I appreciate Mr. Adewale Saheed, Mr. Titus Ofoi who actually encouraged me throughout my studies in AUST.

Finally, I must show my appreciation to my family. My Daddy is always there for me in every aspects of my life. I love you Daddy.

1.0 CHAPTER ONE

1.1 INTRODUCTION

The World Health Organization (WHO) estimated that 84 million people will die from cancer from 2005 to 2015 (WHO media center, 2011).

Cancer is the second leading cause of death in the world (Mackay and Mensah, 2004). It is second only to cardiovascular diseases (Mackay and Mensah, 2004; Boyle and Levin, 2008) and is likely to become the leading cause of death globally by 2030, if the current trends continue (Boyle and Levin, 2008).

The biggest problem lies on the possibility of early stage detection due to the fact that the available resources are limited in demand to many part of world. Also, the existing methods of treatment are based on surgical procedures, radiation therapy, including bulk systemic chemotherapy, that have severe side effects. Further, the current methods of bulk system cancer treatments involve the use of toxic chemical compounds that kill normal /healthy cells, as they circulate through the body. There is, therefore, a need for alternative approaches that can reduce the killing of normal or healthy cells during the cancer treatments (Hildebrandt, et al., 2007).

The field of controlled release has since been born out of this motivation to develop systems that release drugs in a controlled and effective manner. This can be appreciated by examining Figure 1.1. It shows the changes in the blood plasma levels following a single dose administration of a therapeutic agent. This figure shows the blood plasma level rises rapidly and later decays exponentially as drug is metabolized and excreted from the body (Needham and Dewhirst, 2001). Moreover, the figure shows the drug concentrations above which the

drug produces undesirable/toxic side effects above a toxic drug concentration level. The therapeutic window is the difference between these two levels, which is usually based on a dose-response of the median 50% of a population (Jorge and Allan, 2004).

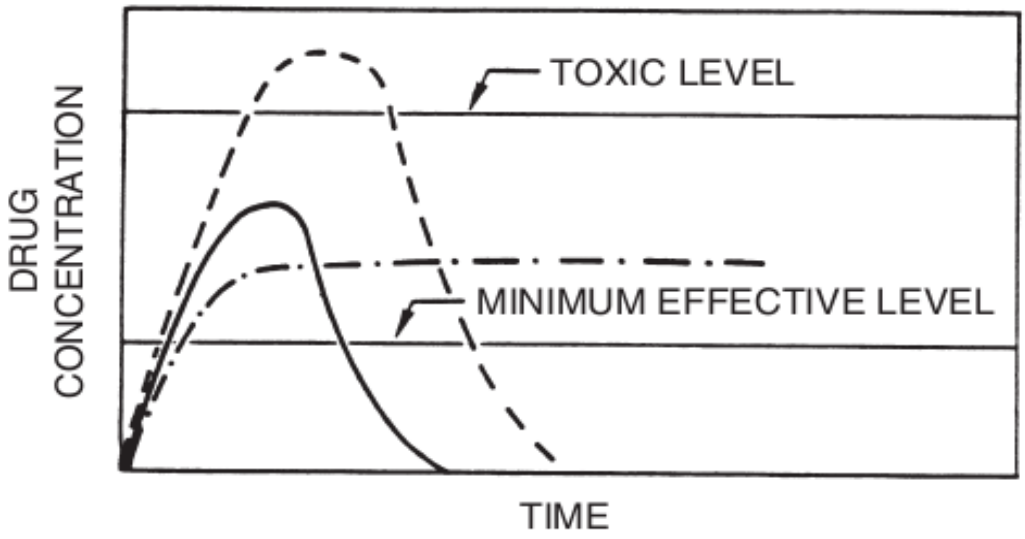

Figure 1.1 Drug concentration following absorption of therapeutic agent as a function of time (—) safe dose, (– – –) unsafe dose, (– · –) controlled release. Reprinted from Roseman, T. J., and Yalkowsky, S. H. in Controlled Release Polymeric Formulations, D. R. Paul and F. W. Harris (eds.). ACS Symposium Series 33, American Chemical Society, Washington DC, pp.33–52.

1.2.1 Implantable BioMEMS

Implantable Bio-Micro-Electromechanical Systems (BioMEMS) represent a new class of devices that can be used to provide localized cancer drug delivery (Oni et al., 2011). They can be inserted in regions that surround cancer tissue, and used surgical drugs, in ways that reduce the short and long term effects of bulk chemotherapy. Implantable BioMEMS typically contain a drug reservoir that can be used to provide drugs locally to tomor sites (Jorge and Allan, 2004). The delivery can be achieved by a number of mechanisms. They include: Polymer drug

release mechanisms can be developed by incorporating swelling hydrogels as the membrane covers for the micro reservoirs; generating sufficient pressure to move the drugs; enough displacement to achieve a desire flow rate and electromechanical response of a polymer material to an electric field. The drug release kinetics relates to the surface properties, liquid uptake behavior and, swelling diffusion.

1.2.2 Cancer and Cancer Statistics

According to the National Cancer Institute, cancer can be thought of as an uncontrolled cellular growth that is caused by the malfunction of specific genes that are responsible for regulating cell growth and division (Figure1.2). This malfunction is attributed to changes in deoxyribonucleic acid (DNA) sequence, and mutation of the genes. It is projected by World Health Organization (WHO) that Global cancer rates could increase by 50 % to 15 million by 2020 (Kheihues et al., 2003).

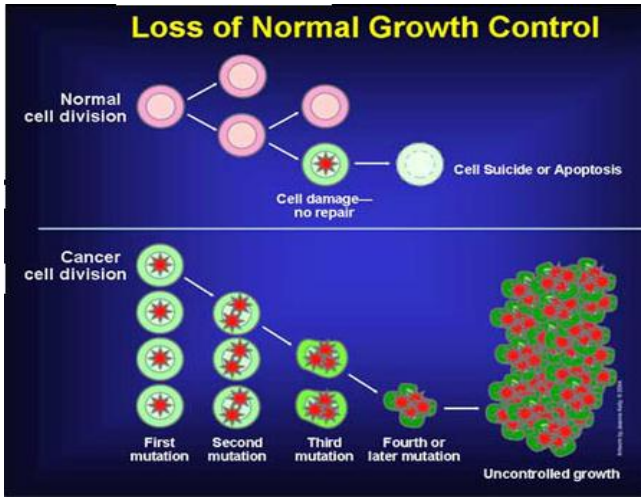

Figure 1.2: Shows the growth rate of cancer cells compared with the normal cell growth.

The incidence of different types of cancer that are observed in men and women is summarized in Table 1.1, which is taken from (GLOBOCAN, 2008).

Table 1.1: World 10 Most frequent cancer in men and women in 2008

Commonest in Men			**Commonest in Women**			**Both Cases**		
Type of cancer	***Number***	***%***	***Type of cancer***	***Number***	***%***	***Type of cancer***	***Number***	***%***
Lung	1,095,000	16.5	Breast	1,383,000	22.9	Lung	1,608,000	12.7
Prostrate	913,000	13.8	Colorectum	570,000	9.4	Breast	1,383,000	10.9
colorectum	663,000	10.0	Cervix uteri	529,000	8.8	Colorectum	1,233,000	9.7
Stomach	640,000	9.6	Lung	513,000	8.5	Stomach	989,000	7.8
Liver	522,000	7.9	Stomach	349,000	5.8	Prostrate	913,000	7.2
Oesophagus	326,000	4.9	Corpus uteri	287,000	4.8	Liver	748,000	5.9
Bladder	297,000	4.5	Ovary	225,000	3.7	Cervix uteri	529,000	4.2
Non-Hodgkin lympoma	199,000	3.0	Liver	225,000	3.7	Oesophagus	482,000	3.8
Leukaemia	195,000	2.9	Thyroid	163,000	2.7	Bladder	386,000	3.0
Liporal cavity	170,000	2.6	Non-Hodgkin lymphoma	156,000	2.6	Non-Hodgkin lymphoma	355,000	2.8

Source: (GLOBOCAN, 2008), http://globocan.iarc.fr/glossary.htm

This shows that breast cancer is the second leading cause of death in women diagnosed with cancer. The forecasted changes in population demographics in the next two decades suggest that even if current global cancer rates remain unchanged, the estimated incidence of 12.7 million new cancer cases in 2008 (Ferley et al., 2010) will continue to rise to 21.4

million by 2030, with almost two thirds of all cancer diagnoses occurring in low- and middle-income countries (IARC, 2011).

Recent reports from the American Cancer Society researchers estimated 1,529,560 new cancer cases and 569,490 deaths from cancer in 2010 (Ahmedin et al., 2010). In the United States, the incidence of breast cancer in women is on the increase. This was released after following successful screening exercise done in some developed nations (Hannah et al., 2003), including the United Kingdom, Denmark, the Netherlands, and Norway (Parkin et al., 2000).

The breast cancer incidence in women that obtained mammograms increased from 32 to 63 % in women of ages within 40 to 49 between 1987 and 1998. Also, for women between the ages of 50 and 64, the incidence of breast cancer increased from 31 to 73 %, upon receiving a mammogram, during the period between 50 and 64 (Angela, 2008).

The increased incidence of breast cancer is attributed partly to risk factors such as second hand smoking (Miller et al., 2007), fatty diets and or obesity (IARC Press; 2002; Kerlikowske, 2008), the use of hormones for birth control (Chlebowski et al., 2009;), delay or refraining from child birth in Western or developed countries (Albrektsen et al., 2005; Lambe et al., 1994), oral contraceptives (Collaborative Group, 1996), excessive alcohol consumption (Baan et al., 2007; Kushi et al., 2006; Cummings et al., 2009), genetic factors (Lichtenstein et al., 2000; Chen et al., 2007; Saslow et al., 2007), and previous exposure to radiation treatments (American Cancer Society, 2009).

However, in the case of developing countries, where the lifestyles are different, reasons for the increased incidence of cancer are not fully understood. However, it is anticipated that the incidence of breast cancer will continue to increase in developing nations, as they

experience economic growth that increases incidence of the risk factors associated with the lifestyles in developed nations.

One way of managing the increased incidence of breast cancer is to reduce the side effects associated with bulk systemic treatment by bulk systemic chemotherapy. This may be achieved by introducing an implantable drug delivery system into a region in which cancer tissue has been removed by surgery (Figure 1.1).

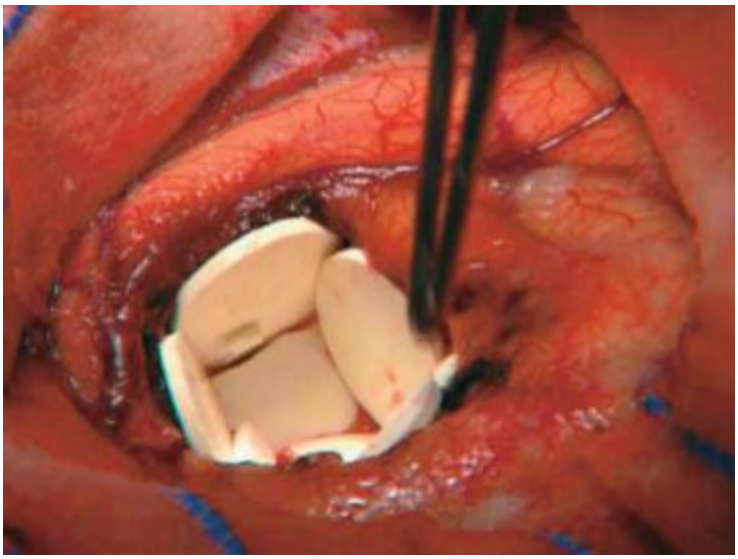

Figure 1.3 polymer implants loaded with BCNU are lined in a human brain tumor resection cavity.

The loaded drug is gradually released when the polymer wafers dissolve away (Hildebrandt, et al., 2007).

The drug delivery system can then release cancer drugs locally into the tissue surrounding the device. In this way, any remaining cancer cells or tissue can be killed, as the eluted drug flows into the surrounding tissue. Since the delivery of the drug is localized, the total quantity of drug, that is needed to have a therapeutic effect, is reduced significantly.

Hence, the potential side effects associated with localized cancer drug delivery should be much lower than those associated with bulk systemic chemotherapy (Oni et al., 2010).

1.2.3 Scope of Work

The primary objective of this work is to develop an implantable BioMEMS device for localized treatment of breast cancer. The materials issue associated with localized drug release will also be elucidated. The research will be carried out in the following steps:

- Poly-di-methyl-siloxane packages with well-controlled micro-channels and drug storage compartments will be fabricated along with a drug storing polymers that will be produced from non-resorbable Poly(N-isopropylacrylamide)(PNIPA) and comonomers of (alkymethacylate and Acrylamide (AM)) and resorbable starch composites reinforced with PNIPA.
- The swelling and fluid release characteristics of the polymers and polymer composites will be studied using bromophenol blue and the cancer drugs, paclitaxel^{TM}. The mechanisms of drug release will be elucidated at temperatures that are relevant to cancer treatment.
- The localized release of the bromophenol blue and paclitaxel^{TM} will then be studied under *in-vitro* conditions. The experiments will establish the drug release rates from micro-channels, of different lengths. A combination of diffusion and micro-fluidics concept models will then be used to model the fluid flow through the micro-channels in the implantable device.

1.2.4 REFERENCE FOR CHAPTER ONE

- Ahmedi Jemal, Rebecca Siegel, Jiaquan Xu, Elizabeth Ward, (2010), American Cancer Society researchers, Cancer Statistics, 2010, a cancer journal for clinicians. Abstract.
- AJCC Cancer Staging Manual. 6th ed. New York: SpringerVerlag; 2002.
- Albrektsen G, Heuch I, Hansen S, and Kvale G. Breast cancer risk by age at birth, time since birth and time intervals between births: exploring interaction effects. Br J Cancer. 2005;92:167-75.
- American Cancer Society. Cancer Facts & Figures 2009, Atlanta, GA: American Cancer Society; 2009.
- Angela Logomasini, (2008), The Competitive Enterprise Institute, "The Cancer Trend", (www.cei.org) 202-331-1010
- Baan R, Straif K, Grosse Y, et al. (April 2007), "Carcinogenicity of alcoholic beverages". Lancet Oncol, 8(4): pp292-293.
- Calle EE, Feigelson HS, Hildebrand JS, Teras LR, Thun MJ, Rodriguez C. (Jan 20 2009), "Postmenopausal hormone use and breast cancer associations differ by hormone regimen and histologic subtype". Cancer.;115(5):pp936-945.
- Chen S, and Parmigiani G, (2007), "Meta-analysis of BRCA1 and BRCA2 penetrance". J Clin Oncol, 25: 1329-33.
- Chlebowski RT, Kuller LH, Prentice RL, et al. Breast cancer after use of estrogen plus progestin in postmenopausal women. N Engl J Med. Feb 5 2009;360(6):pp573-587.
- Collaborative Group on Hormonal Factors in Breast Cancer. Breast cancer and hormonal contraceptives: collaborative analysis of individual data on 53,297 women with breast cancer and 100,239 women without breast cancer from 54 epidemiological studies. Lancet. Jun 22 1996;347(9017):1713-1727.

- Cummings SR, Tice JA, Bauer S, et al. Prevention of breast cancer in postmenopausal women: approaches to estimating and reducing risk. J Natl Cancer Inst. Mar 18 2009;101(6):384-398.
- Ferlay J et al. Estimates of worldwide burden of cancer in 2008 (GLOBOCAN 2008). International Journal of Cancer, 2010, Vol.127:pp2893–2917.
- Hannah et al., "Annual Report to the Nation on the Status of Cancer, 1975–2000, Featuring the Uses of Surveillance Data for Cancer Prevention and Control," Journal of the National Cancer Institute 95, no. 17 (2003): 1276–99.
- Hartmann L. C., T. A. Sellers, D. J. Schaid, T. S. Frank, C. L. Soderberg, D. L. Sitta, M. H. Frost, C. S. Grant, (2003).
- Hildebrandt B., P. Wust in: W.P. Ceelen (Ed), (2007), Peritoneal Carcinomatosis: A Multidisciplinary Approach, Springer, New York, p. 185.
- International Agency for Cancer Research (IARC)(2002), "IARC Handbook of Cancer Prevention, Volume 6: Weight control and physical activity". Lyon: IARC Press; 2002.
- International Agency for Research on Cancer (IARC), (2011), "Cancer incidence and mortality worldwide: (IARC Cancer Base No.10)", Lyon.
- Jorge Heller and Allan S. Hoffman (2004), An Introduction to Materials in Medicine 2nd Edition, 2004, Elsevier Inc., pp 628-637.
- Kerlikowske K, Walker R, Miglioretti DL, Desai A, Ballard-Barbash R, Buist DS (Dec 3, 2008), "Obesity, mammography use and accuracy, and advanced breast cancer risk", J Natl Cancer Inst,100(23), pp1724-1733.
- Kushi LH, Byers T, Doyle C, et al., (Sep-Oct 2006), "American Cancer Society Guidelines on Nutrition and Physical Activity for cancer prevention: reducing the risk of cancer with healthy food choices and physical activity". CA Cancer J Clin.;56(5):pp254-281; quiz 313-

254.

- Lambe M, Hsieh C, Trichopoulos D, Ekbom A, Pavia M, and Adami HO. Transient increase in the risk of breast cancer after giving birth. N Engl J Med. 1994; 331:pp5-9.
- Lichtenstein P, Holm NV, Verkasalo PK, et al (Jul 13, 2000), "Environmental and heritable factors in the causation of cancer--analyses of cohorts of twins from Sweden, Denmark, and Finland", N Engl J Med.; 343(2):pp78-85.
- Mackay J., Mensah G.A. (2004), The Atlas of Disease and Stroke, WHO Non-serial Publication.
- Needham D. and Dewhirst M.W. (2001), "Advanced Drug Delivery Reviews", Vol. 53, pp285– 305.
- Oni Y., C. Theriault, A. V. Hoek, W. O. Soboyejo, (2011), "Effects of temperature on diffusion from PNIPA-based gels in a BioMEMS device for localized chemotherapy and hyperthermia", Journal of Materials Science and Engineering C, www.elsevier.com/locate/msec, Priceton University USA. p.2-5.
- Parkin, Bray, and Devesa, "Cancer Burden in the Year 2000."
- Paul Kleihues, Gro Harlem Brundtland, Bernard W. Steward (2003), International Agency for Researched on Cancer (IARC), WHO media centre, World Cancer Report (2003), p351.
- Peter Boyle and Bernard Levin (2008), "The World Cancer Report by World Health Organization"
- Rebecca Siegel, Elizabeth Ward, Otis Brawley, Ahmedin Jemal, (2011), "The Impact of Eliminating Socioeconomic and Racial Disparities on Premature Cancer Deaths", Cancer Statistics, American Cancer Society.

- Saslow D, Boetes C, Burke W, Harms S, Leach MO, Lehman CD, Morris E, Pisano E, Schnall M, Sener S, Smith RA. Warner
- Stewart BW, Paul Kleihues P. (2003) World Cancer Report. Lyon, France, International Agency Research on cancer.
- Tiwari et al, 2004, "Data on the number of deaths obtained from the national cancer control and prevention" Breast cancer facts and figures 200-2010.
- Yaffe E, Andrews M, and Russell CA. American Cancer Society guidelines for breast screening with MRI as an adjunct to mammography. CA Cancer J Clin. 2007;57: 75-89.
- Young JL Jr, Roffers SD, Ries LAG, Fritz AG, Hurlbut A, eds. SEER Summary Staging Manual - 2001: Codes and Coding Instructions. Bethesda, MD: National Cancer Institute; 2001. NIH Pub. No.01-4969.

CHAPTER TWO

2.0 Literature Review

2.1 Introduction

The incidence of cancer in the world today has is one of the public health problems that has fueled the philanthropists, the sponsors, and researchers to actively get involved to find better strategies on early detections and treatments of cancer. The development of drug delivery devices, a part of which this work addresses, has been the focal point of research in recent years (Hoffman and Afrassiabi, 1987; Oni et al, 2011).

In recent years, significant efforts have been made to develop bio-micro-electro-mechanical systems (BioMEMS) for the localized treatment of cancer (Oni et al., 2010). It has been reported, that cancer is currently responsible for 20,000 deaths per day, and 7.6 million incidences per year across the globe (Cutierrez, 2008). From the same report, 2.9 million cases are expected to have occurred in the developed world, while 4.7 million remained the situation in the less developed countries.

According to the American Cancer Association; breast, colorectal, and lung cancer are the most common forms of cancer in women in developed countries, while in developing countries, breast cancer still remains as the most common form of cancer among women, followed by cervical, and stomach cancer. Among cancers in men, the most prominent type in developed nations is prostate cancer, followed by lung, and colorectal cancers, whereas stomach, lung, and liver cancers stands the most common forms of cancer among men in the less developed world (Melissa et al, GLOBACAN, 2008), on the report entitles Global Cancer facts and figure.

This chapter presents a review prior work and the underlying materials concepts that are relevant to the development of BioMEMS for cancer treatment. These include: swelling and drug delivery kinetics that are relevant to implantable drug delivery systems, as well as heat diffusion for localized hyperthermia. The chapter also presents drug delivery devices, the use of micro-fluids and hydrogels in localized cancer drug delivery, and the use of polylactic acid (PLA)/ Polyglycolic acid (PGA) composites in localized cancer treatment. Finally, the role of surface coatings and surface texture is discussed for the development of implantable devices that adhere and integrate well with biological tissue.

Prior work (Jondavid, 2006) has shown that breast cancer typically starts in the breast, within thin tubes called the ducts. Early breast cancer is still within the breast or in glands under the arms known to be the lymph nodes (figure 2.1a, b). During breast feeding, breast milk is carried by the ducts, from the milk-producing glands, to the nipple. In the case of invasive breast cancer, the cancer cells spread beyond the ducts and are found in the fatty tissues of the breast. It eventually spreads throughout the body, when it breaches the cell membranes. When this occurs, the cancer cells can be carried in the bloodstream to induce metastases, especially in the lungs and in the bone (Jondavid, 2006).

a

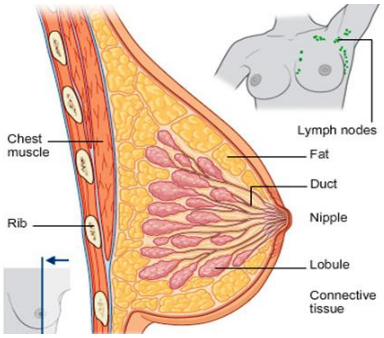

b

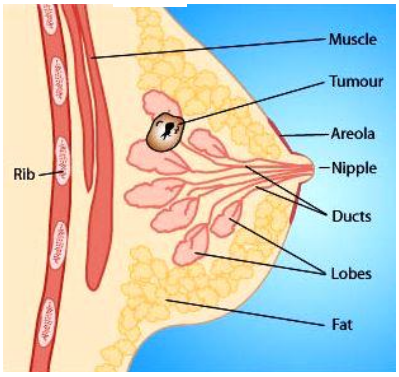

Figure 2.1 (a) Illustrating the anatomy of a woman breast; (b) the position of tumor located within the breast. Adapted from (Paul Crea St. Vicent's Clinic, 2007).

In Most breast cancers usually arise from the lining of the milk ducts and some arises from the milk glands found within the breast lobes and the most common site is the upper outer part of the breast.

2.2 Cancer Statistics

Cancer is reported to be increasingly causing morbidity and mortality in all regions across the globe (Ala, 2010). The increasing population growth suggested that, even if the current trends in cancer should remain unchanged, cancer would still contribute to 21.7 million new cases in 2008 (Ferlay et al, 2008). Moreover, the statistics indicated that two thirds of the entire global incidence of cancer would occur in low and middle income nations ((IARC, 2011).

The American Cancer Society report in 2008 projected 715,700 new cancer cases in Africa, 1,034,300 cases in Western Europe, 3,720,700 new cases in Eastern Asia, South-Eastern Asia is 725,600, South-Central Asia, indicating 1,423,100, out of 12,667,500 worldwide estimates contributing to one death in eight. Hence, cancer deaths will be more than the deaths due to AIDS, tuberculosis, and malaria combined (GLOBACAN, 2008). The figure, for Africa, was low which may be due to incomplete report on cancer statistics. Early detection and secondary prevention via screening is, therefore the key to detection of pre-cancerous cells or tissue.

2.3 The Symptoms of Breast Cancer and Problems with Existing Treatment Methods

Although the origin of cancer is not fully understood, cancer is generally associated with an acceleration of cell dynamics, and the propagation of errors in the deoxyribonucleic acid

(DNA) to ribonucleic acid (RNA) transcription process. It is very unusual for breast cancer to produce symptoms in its early stage. This gives rise to late detection and treatment, and becomes a challenge when cancer reaches the metasteses stage.

2.3.1The symptoms of cancer include;

- Lymph thickening of breast tissue
- Swelling in the armpit or around the collar bone
- Changes in size or shape of the breast
- Changes in skin texture such as puckering or dimpling
- Discharge from nipples such as blood
- Constant pain in breast or armpit
- An inverted nipple (changes in the nipple where the nipple is pulled back into the breast
- Redness or a rash on the skin or around the nipple

2.3.2 Current Cancer Treatment Methods and Their Challenges

The existing bulk systemic cancer treatment methods include; surgery, radiation, chemotherapy, hormones, and immunotherapy. However, the side's effects of these current treatments are severe. Surgery has been recognized as a way of treating cancer. However, it can disfigure the patient. Furthermore, there are no guarantees that all of the cancer cells or tissue will be removed by surgery. Radiation on the other hand can be damaging to the local healthy organs and tissues.

The use of bulk systemic chemotherapy as a cancer treatment method also has some major challenges (David and Mark, 2001). This is because only one tenth of one percent of the

injected drugs reaches the desired tumor sites. Hence, most of the injected drugs kill or damage healthy cells or tissues that do not require chemotherapy (Chaplin et al., 1998). This causes undesirable short and long term side effects (David and Mark, 2001).

Some researchers have explored the potential of liposomes to serve as cancer drug carriers (Gregoriadis, 1976). Conventional liposomes have been evaluated chemically and are used in treating Kaposi sarcoma (Figure 2.2). However, they failed to release drugs in a controllable manner to tumors (David and Mark, 2001). The applications of local hyperthermia where an external power such as microwaves, radio frequency and or ultrasound is applied to the increase the temperature above the 37^{o}C to 42^{o}C.

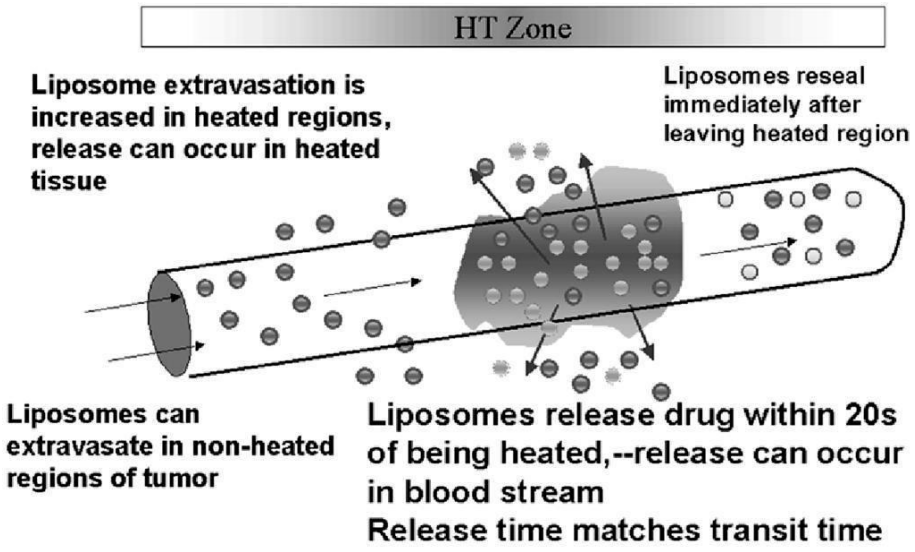

Figure 2.2 Summary of the mechanisms underlying liposome-based drug delivery to tumors for the heat-sensitive liposome system (David and Mark, 2001).

2.4 Cancer Drug Delivery

Progress has been made in the development of drug delivery systems for localized cancer treatment. Meanwhile, the drawbacks accompanying bulk systemic chemotherapy have

inspired current efforts toward the development of new approaches to enhance localized chemotherapy (Oni and Soboyejo, 2010). This section presents a review of drug delivery approaches that are relevant to localized treatment. The current developed drug delivery devices includes: local chemotherapy; controlled cancer therapeutics; liposomal systems; transdermal drug delivery patches; microchips; micro-pumps; microspheres; polymer conjugates (Figure 2.3a), and a multiwell silicon-based drug-release devices (Figure 2.3b).

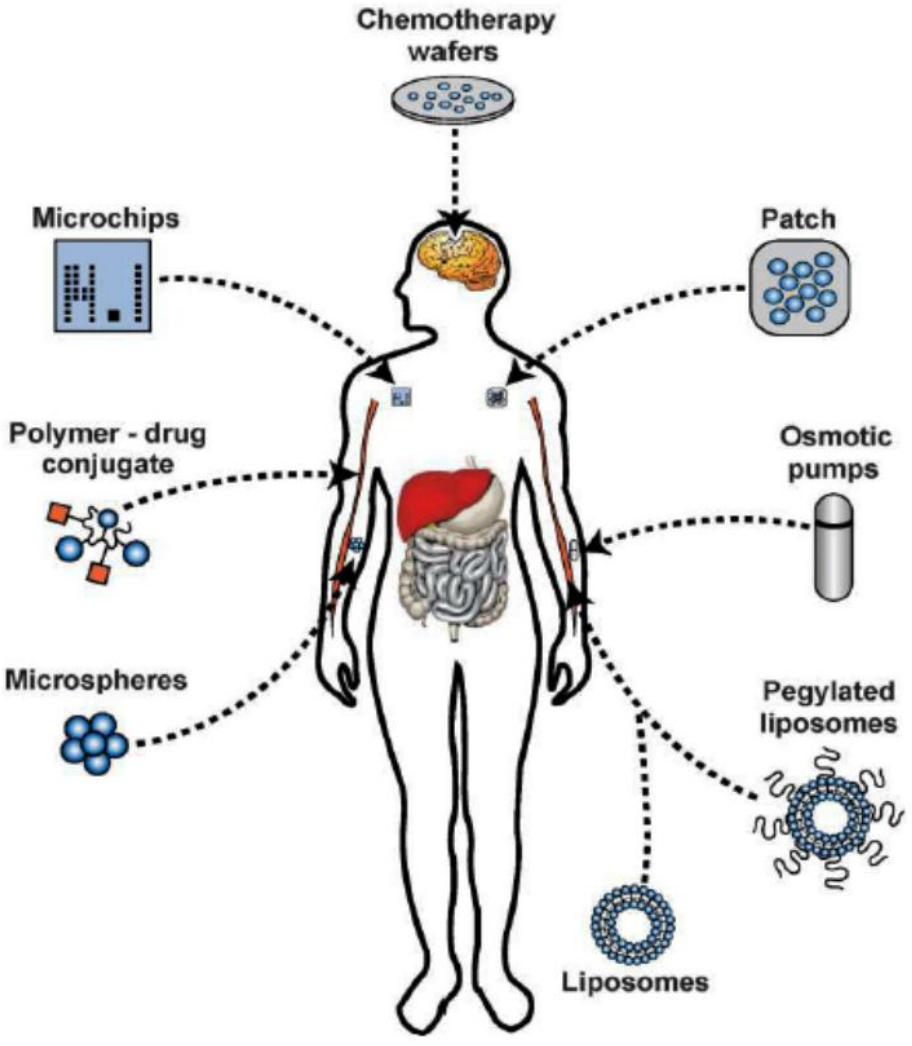

Figure 2.3a A variety of different delivery strategies that are currently being used or in testing stage to treat human cancers (Adapted from Hildebrandt et al., 2007).

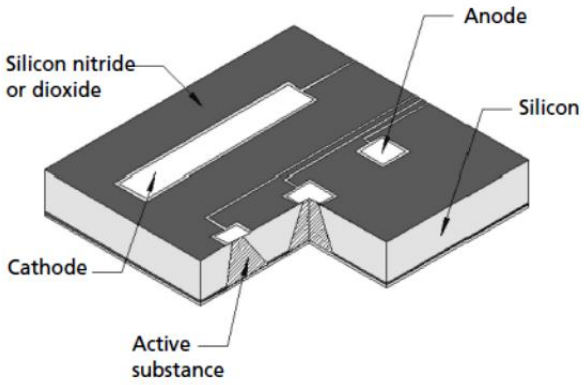

Figure 2.3b Multiwell silicon-based drug-release device, adapted (adapted from Santini et al., 1999).

2.4.1 Micropumps

Micropumps, as well as microneedles, are microfluidic products that are used in the biomedical field, especially in drug delivery. Micropumps are classified into two groups, depending on the actuation mechanisms involved in the device operation. For instance, there are those that operate mechanically (moving parts are involved), and others that are non-mechanical. A comprehensive review of prior work on micropumps has been presented by Muhammed et al., 2011. This summarizes microfluidic design approaches, their performance parameters, working principles, fabrication techniques, and safety issues.

Flow is usually controlled, although some devices may rely on natural driving forces (such as diffusion and osmosis) to deliver drug concentrations locally within the therapeutic window.

There has been progress in recent times toward developing micro-fluid transdermal drug delivery devices (Ashraf, 2010). A schematic illustration of a transdermal drug delivery system is shown in Figure 2.4. In such devices, the actuator provides the necessary force

required for fluid to flow in the device. The valve also plays a significant role in micro-pumps, as it controls the flow of fluid through the device and closes when necessary.

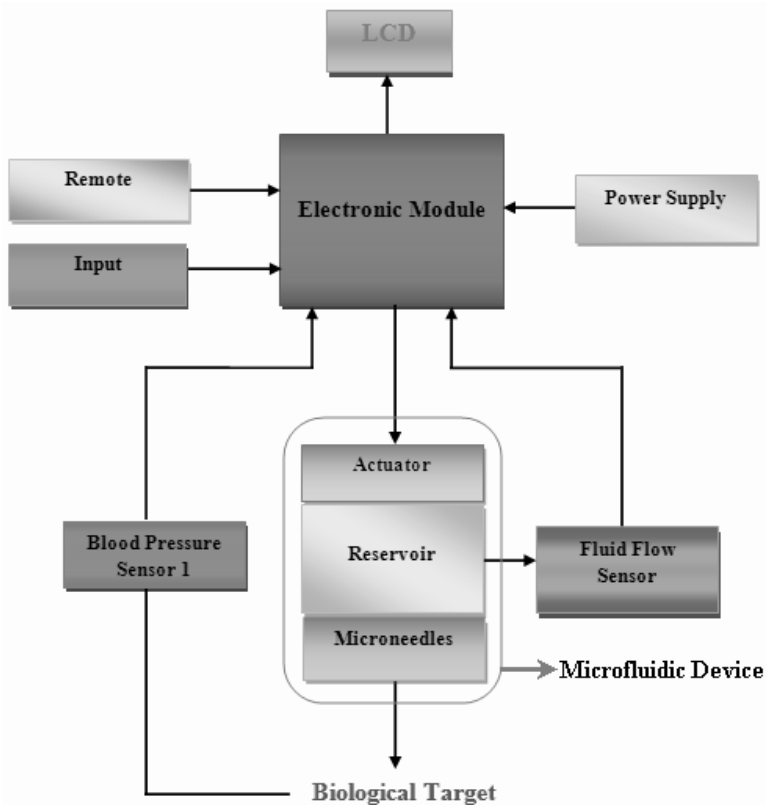

Figure 2.4 Schematic illustration of transdermal drug delivery system: adapted (Muhammad et al., 2011).

2.5 Drug Delivery Polymers

In recent years, there have been increasing efforts to develop biodegradable polymers for drug delivery systems. These has favored because such syste4ms do not require surgical removal, once the drug supply is depleted. There are efforts by major chemical companies to make monomers and polymers that are readily more accessible. The mechanism controlling biodegradation of a polymer is basically hydrolysis of the ester linkages, which gives an idea on the role played in *vivo* performance of the lactide or glycolide materials.

Moreover, the crystallinity and intake of water are also factors that can determine the rates of the in vivo degradation of the polymer.

Poly-caprolactone and its copolymers have been explored for controlled drug delivery. This form compatible blends with some other polymers (Brode et al., 1972; Koleske ,1978).

Natural and Synthetic polymers mostly are used for drug delivery and they have minimal effect on the biological systems after their integration into the body. The degradation of *in vivo* is at a well-defined rate to nontoxic and this has been long explored to have readily excreted degradation products (Mark and Robert 1990).

But a natural polymer remains more attractive since they are readily available. More to the point, the natural polymers are relatively inexpensive and they can be chemically modified.

2.6 Gels

Gels are polymeric networks that are held together by secondary bonds. They can undergo structural changes due to changes in PH, temperature and environment (Kaifeng et al., 2007). Hydrogels are covalently bonded polymeric networks that contain water. They are formed by simply reacting one or more comonmers. Hydrogels can also be physically cross-linked from entanglements, associated bonds such as hydrogen bonds/ strong Van der Waals interactions between chains (Peppas, 1987).

2.6.1 Poly (N-Isopropylacrylamide) (PNIPA) Hydrogels

A considerable progress has been made to understanding PNIPA which led to the discovery of the volume phase transition of PNIPA gels (Hirokawa and Omodaka, 1984). Smart hydrogels have been studied in recent years to harness their swelling behavior and the release of fluid in their response to environmental stimuli such as temperature, pH, electric field and solvent composition (Afrassiabi, 1987; Schmaljohann, 2006; Farmer et al, 2008). Since PNIPA gels can be used to store and release controlled amounts of drugs which, they have the potential for applications in drug delivery systems (Soppimath, 2002, Jeong et al., 2002).

Thermo-sensitive hydrogels have recently been explored for their potential in drug delivery (de Las et al, 2005). PNIPA is thermo-sensitive hydrogel with a lower critical solution temperatures (LCST) of about 32˚C in an aqueous solution especially when PNIPA is been cross-linked (Shild, 1992). PNIPA gel synthesis involves polymerization under heterogeneous and homogeneous conditions. It exhibits a swelling transition around 32˚C (Michal et al., 2006). It is also noted that 32˚C is close to the physiological body temperature body of humans (37˚C). This makes PNIPA gels attractive for potential applications in controlled release. A study conducted shows that polyelectrolytes have an influence on the lower critical solution temperature of PNIPA hydrogels (Yoo et al., 2000). It has also been reported that the LCST of PNIPA is dependent on PH and its LCST would increase with an increase in pH (Yoo et al, 2000). Moreover, crosslinking NIPA with acrylamide helps to effectively increase the LCST (Oni et al., 2011).

When PNIPA is heated above a critical temperature of 32°C-35°C in water, it undergoes a reversible temperature phase transition from a swollen hydrated state to a shrunken dehydrated state, thereby losing about 90% of its mass (Schild, 1992).

This characteristics behavior of PNIPA (expulsion of liquid) has led many researchers to study its potential for applications in controlled drug-delivery (Zhang et al., 2001).

However, further work is needed to explore new ways of improving the swelling and drug release kinetics of PNIPA hydrogels (Park, 1999; Pelton, 1986; Fu et al., 2010; Oni et al., 2010). It has also been shown that PNIPA has the ability to store and release drugs. Furthermore, recent work has shown an improvement in the swelling performance of PNIPA hydrogels by forming interpenetration polymer networks inside the PNIPA hydrogel (Zhang et al., 2005).

In spite of the numerous advantages of hydrogels, they have poor mechanical properties. The mechanical properties of hydrogel materials were first developed by Flory (Kaifeng et al., 2007). PNIPA gels have low strength and low modulus, especially in the swollen state. This has led to the development of new gel composites that consist of polyurethane foams and PNIPA (Kaifeng et al., 2007).

2.6.2 Polyacrylamide Gel Co-Polymers

The acrylamide (AM) monomer can be cross-linked with small amounts of Methyl bisacrylamide (MBA) by polymerization. MBA is used as a crosslinked agent because of its two acrylamide molecules linked by a methylene group. The AM monomer usually polymerizes in a head-to-tail manner into long chain which contributes to the building of a growing chain. This also initiates a second site for chain extension. The polymerization of

AM is characterized by free-radical catalysis (John, 1996), hence ammonium persulfate (APs) and the base *N,N,N',N'*-tetra-methyl-ethylene-diamine (TEMED) can serve as initiators for the process. Furthermore, TEMED catalyzes' the decomposition of the persulfate ion to give a free radical (i.e a molecule with an unpaired electron) (John, 1996).

$$S_2O_8^{2-} + e^- \rightarrow SO_4^{2-} + SO_4^- \tag{2.1}$$

The polymerization can be represented (equation 2.2). Suppose we take the free radical as $\dot{R}$ and acrylamide monomer molecule to be M. This implies:

$$R + M^{\cdot} \rightarrow R\dot{M}$$

$$R\dot{M} + A^{\cdot} \rightarrow RM\dot{M}$$

$$RM\dot{M} + M \rightarrow RMM\dot{M}, \qquad \text{and so forth} \tag{2.2}$$

This develops longer acrylamide chains, especially when MBA molecule is introduced into solution.

2.6.3 Hyperthermia

The phrase "hyperthermia" refers to the techniques of applying heat to improve cancer treatment. Hyperthermia could be used in conjunction with conventional techniques to improve the outcomes of cancer treatment. For example, the synergy of hyperthermia combined with radiotherapy, and chemotherapy can effectively kill cancer cells within the framework of multimodal treatments (Hildebrandt et al., 2002).

Hyperthermia can be done locally or regionally depending on the system. The types of hyperthermia include whole-body hyperthermia (HBH), hyperthermia isolated limb perfusion (HILP), and hyperthermic periotoneal perfusion (HPP) (Hildebrandt et al.,

2002). Prior work gives suggestions on the effectiveness of using hyperthermia in clinical treatment of cancer (Hildebrandt et al., 2000; Issels et al., 1990; Wust, 1996; Rau et al, 2000; Oni et al., 2011).

Hyperthermia on its own has low efficacy to be used to conquer cancer. This current work aimed to combine hyperthermia with chemotherapy to deliver drugs locally to the target tumor using loaded thermo-sensitive PNIPA gels. Experiments with hyperthermia on *in-vitro* and animals have demonstrated effective cell deaths within temperatures of 41 to 47˚C (Urano et al, 1999; Dewey, 1994; Dewhirst, 1997). Hyperthermia could enhance tumor blood flow which will intend improve the supply of nutrients and oxygen under *in-vivo* condition. However, the result from in-vivo sometimes does not agree well with *in-vitro* observations made even under a controlled condition (Haim, 1980). This may be due to the interactions between different physiological factors that are absent in the *in-vitro* environment.

2.6.4 Poly (lactic acid) (PLA)/ Poly (glycolic acid) (PGA) resorbable gels

Greater part of biodegradable polymers studied in recent times belongs to the polyester family: Poly (lactic acid) (PLA) and Poly (glycolic acid) (PGA). Significant impacts of biodegradable polyesters have been made in medicine for the past century. PLA, PGA, and their copolymers have countless clinical applications (Yong and Kinam, 2001; Gareth, 2004). The polymer chains are degraded hydrolytically and enzymatically. Their structures are shown in Table 2.1. PGA is normally synthesized by the rigid opening of glycolide and that gives the reason why it is sometimes referred to us poly (glycolide). PGA is a highly insoluble polymer and it is unremarkable when used as a copolymer with PLA.

Table 1Table 2.1 shows the polymer unit structures of PGA and PLA, respectively.

Polymer	Polymer repeat unit structure
Poly(glycolic acid)	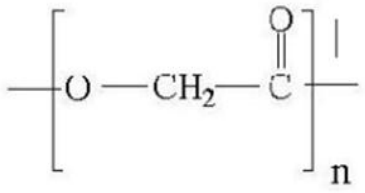
Poly(lactic acid)	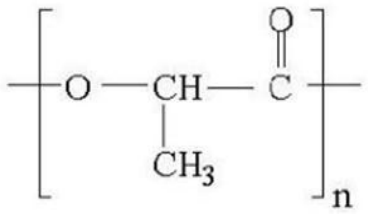

However, these polymers suffer from: poor biocompatibility, the release of acidic degradable products, poor addressability, and loss of mechanical properties on their earlier stages during degradation.

The largest application of PLA/PGA polymers is in drug-delivery systems, resorbable sutures, and other orthopaedic fixation devices such as pins, rods, and screws (Behravesh et al., 1999; Middleton et al., 2000). PGA is also known to be a rigid thermoplastic material with a high crystallinity of (40-50 %). Its glass transition temperature and melting temperature are 36^{o}C and 225^{o}C, respectivelly (Pathiraja and Raju, 2003).

2.6.5 Polydimethylsiloxane (PDMS)

Polydimethylsiloxane (PDMS) is a silicon-based organic polymer (Figure 3.1), that has unusual rheological properties. It is optically clear, and it is also considered to be inert, non-toxic, and biocompatible (American Food and Drug Association approved).

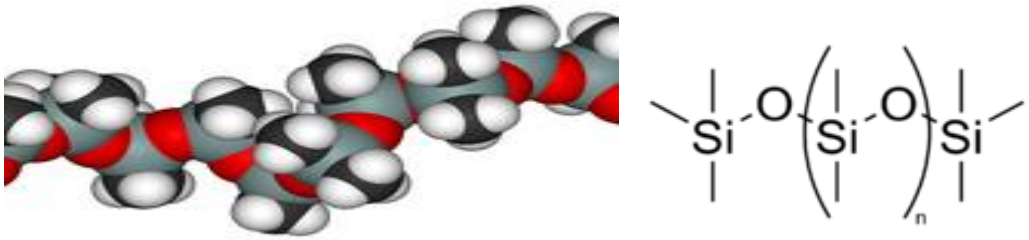

Figure 2.1 Shows a Linear Polydimethylsiloxane (Adapted from Joint Assessment of Commodity Chemicals) (1994) (Report No. 26) ISSN 0773-6339-26.

Biocompatible and inexpensive polymers, such as Polydimethylsiloxane (PDMS), are often materials of choice for the fabrication of microfluidic devices (Oni, 2010).

Some diseases demands repeated administration of drugs over long periods of time, ranging from months to years with precise control for reasons of safety and efficacy. There are challenges for delivery due to the inaccessibility of the target tissue or organ. In view of this, the current work is focused on fabricating fully implantable, self-controlled drug delivery system to treat cancer. The goal is to produce an implantable device that can deliver cancer drugs to breast tumor sites within an African and global context.

The main advantage of localized delivery is that it reduces the amount of drug that is needed to have therapeutic effect (Ali, 2008). Hence, localized drug delivery can reduce the side effects associated with chemotherapy. These can be further reduced by the synergy that can be engineered between localized hyperthermia and localized chemotherapy.

2.7 Swelling / De-swelling Kinetics

2.7.1 Swelling Kinetics

PNIPA gel exhibits a phase transition at about 34˚C (Oni et al., 2011). At this temperature, the gels shrunk significantly and release fluid. The fast response rate of PNIPA to external stimuli has attracted much attention towards their applications in drug delivery (Oni et al., 2011). The swelling or shrinkage of PNIPA gels is usually controlled by the diffusion of water molecules through the gel network (Oh, 1998). Although, this process may be slow, especially near the critical point, the rate of response inversely proportion to the square of the gel size (Tanaka, 1979). Some studies have shown dangling chain structures of PNIPA gels (Yoshida et al., 1995), (Kaneko et al., 1995). This implies the gel would easily collapse and expand when an external stimulus is applied, as a result of the free dangling chain on the side.

Furthermore, PNIPA gels have been shown to have micro or macro-porous networks that enable them to soak in fluid. The adsorption or desorption of water therefore, occurs through the interconnected pore structures by convection (Yual and Oguz, 2005). The macro-porosity of PNIPA gel depends on: the phase separation that occurs during cross-linking; gel synthesis parameters such as temperature and crosslinkage; monomer concentration, and then the pore-forming agent such as the type of the inert diluent used (Okay, 2000). However, the gel preparation temperature appears to exert the greatest influence on the macroporosity within the PNIPA gel network (Yual and Oguz, 2005). This suggests that polymerization below the lower critical solution temperature (LCST) should help achieve the macroporous gel network.

However, prior work (Takata, 2002), has shown that rapid shrinkage of PNIPA gels occurs when the preparation temperature is above LCST. It is also possible to produce fast responsive PNIPA gels at temperatures below freezing point (-18˚C). Poly (ethylene glycol) (PEG) made of various molecular weights have been reported to have improve the fast responsive macroporous PNIPA hydrogels (Cicek, et al., 2003). Zhang et al, 2003 have shown that PNIPA gels can be prepared to achieve higher degrees of porosity by increasing the crosslinker concentrations. The critical crosslinker concentration can possibly cause a heterogenous macroporous PNIPA network structure (Sayil et al., 2002). The process in gelation changes from a homogeneous to heterogeneous which helps with fast the response with the hydrogels.

The swelling performance of the hydrogels is accomplished through a direct weighing, prior to soaking the gels in water at temperatures between 25.5˚C to 51˚C inside a temperature control led water bath. The swelling ratio is given by:

$$S_R = \frac{W_T}{W_O} \qquad (2.3)$$

where W_T is the weight of water in the fully swollen gel at temperature T, and W_O is the weight of the dry gel. Some recent work (Fu and Soboyejo, 2010) uses sodium Alginate in PNIPA gels to improve the swelling ratios. The sodium alginate enhances the interpenetrating polymer network and it is importantly, biocompatible (Atala et al., 1994).

2.7.2 De-Swelling

The de-swelling kinetics of PNIPA can be determined by soaking in water at 25˚C, to equilibrium. The saturated specimens are then transferred into a hot distilled water bath at

about 37- 45˚C (Oni et al., 2010). The re-swelling experiment is carried out by transferring the dried gels into water in a water bath at higher temperatures. This is done after an equilibrium weight is obtained in the swelling measurement back into water at 28˚C. The water uptake in the gels is obtained with the relative gel mass (Yual and Oguz, 2005):

$$M_{rel} = \frac{M_t}{M_s} \tag{2.2}$$

where M_t is the mass of the gel samples at time, t, and M_s is the swollen mass at 28^{o}C. An inorganic phase was incorporated into PNIPA gels to give faster de-swelling kinetics, and also helps to improved mechanical properties of the gels when prepared under homogeneous conditions (Kabra and Gehike, 1991). Homogeneous synthesis conditions could be achieved at temperatures above LCST with the reaction in water. The process creates microphase separation of PNIPA during polymerization, yielding a highly porous product structure. The process favors the acceleration of swelling or de-swelling (Kabra and Gehike, 1991).

2.7.3 Equilibrium Swelling Measurements

Equilibrium swelling measurements are determined by soaking the gels in distilled water at room temperature, 25˚C for two weeks (Yucel and Oguz, 2005). The volume of the gels at the swollen state (V_{eq}) is determined from the measured diameters of the hydrogel samples, using equation 2.3 presented below:

$$V_{eq} = \frac{D}{D_o} \tag{2.3}$$

where D_o and D are the respective diameters of the hydrogels, before and after the equilibrium swelling.

2.5 Drug Release Kinetics and Diffusion Mechanism

Table 2.3 Summary of exponent associated with diffusion mechanisms in drugs eluting from polymeric films (Peppas, 1985).

Table 2.3 Summary of exponent associated with diffusion mechanisms in drugs eluting from polymeric films

Release exponent, n	Drug transport mechanism	Rate (dM_t/dt) as a function of time
0.5	Fickian diffusion	$t^{-0.5}$
0.5 < n < 1.0	Anomalous (non-Fickian) transport	t^{n-1}
1.0	Case-II transport	Zero-order (time-dependent) release
n > 1.0	Super-Case-II transport	t^{n-1}

A number of prior researchers have developed models that provide insights into the mechanism of drug release in hydrogels (Peppas, 1985), (Siepmann and Peppas, 2001; Hedeenqvist et al., 1996). These studies suggest that, the release of solutes is governed by diffusion and viscoelastic behavior of the swollen gels. The released exponent (n) and the dependent constant via diffusion system (k) have been determined (Peppas, 1985):

$$\frac{m_t}{m_\infty} = kt^n \qquad (2.4a)$$

where $\frac{m_t}{m_\infty}$ is the drugs fractional release at time t, k is the constant relating the structural and geometric characteristics of the controlled release device, and n is the release exponent

which indicates the mechanism of drug release. A logarithm equation from equation (2.4a) obtains the release of fluids by a gel given in equation (2.4b):

$$\ln\left(\frac{m_t}{m_\infty}\right) = \ln k + n \ln t \qquad (2.4b)$$

From the linear plots of $\ln\left(\frac{m_t}{m_\infty}\right)$ versus $\ln t$ would give the values of n, k and their corresponding regression coefficient, R^2.

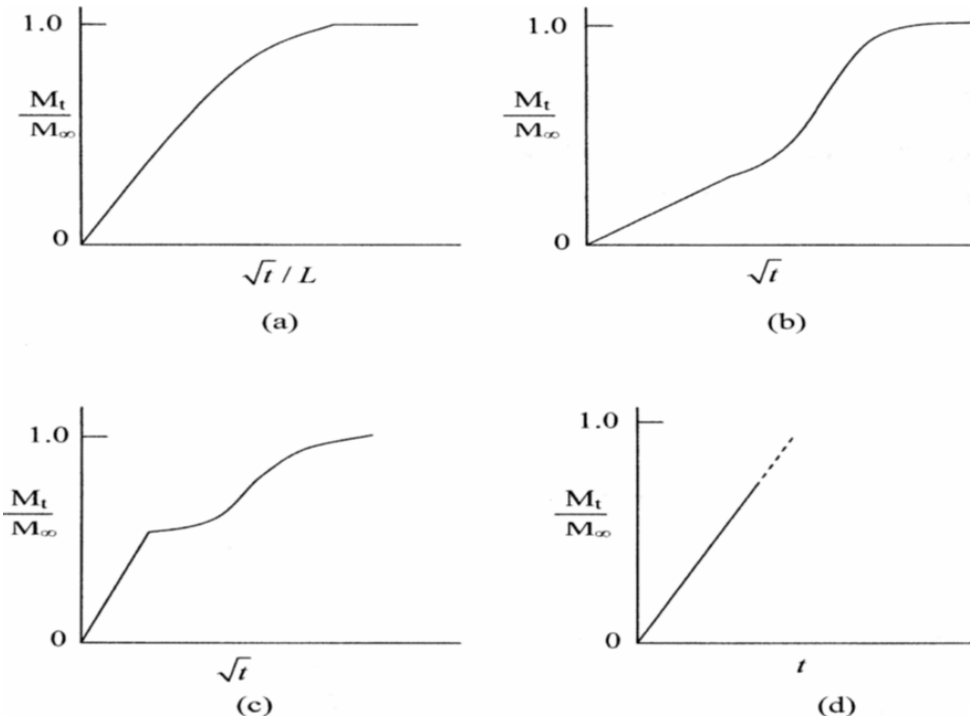

Figure 2.5 Different classes of non-Fickian sorption: (a) classical; (b) sigmoidal; (c) two-step; and (d) Case II (Kee et al., 2005).

2.8 Cell/ Surface Interactions

Efforts have been made from recent research to reduce the factors that can cause loosening of an implant (Dumbleton et al., 2002; Willert et al., 1999). These factors include; the modification and manipulation of the surface chemistry as well as the modification of the implant surface texture. Modifying the surface of the implant is advantageous. It has a

greater impact on the multi-scale, which ranges from chemisorption and surface energies within the atomic scale (Feng et al., 2003), and to surface roughness and texture at the micro-to-meso-scale (Menezes et al., 2003).

Surface texture with proteins such as fibronectin, actin, cinculin, and integrins plays a significant role in cell adhesion (Anselme, 2000). Their interactions also helps to improve cell growth and differentiation (Anselme, 2000; Burridge et al., 1988; Lauffenberger et al, 1996). Experimental studies of the effects of surface texture on the interactions between human osteo-sarcoma (HOS) cells and Ti-6Al-4V have been studied by prior work (Chen et al., 2006). This shows that contact guidance and improved cell or surface integration can be promoted by laser microgrooves and separations that are comparable to the cell size.

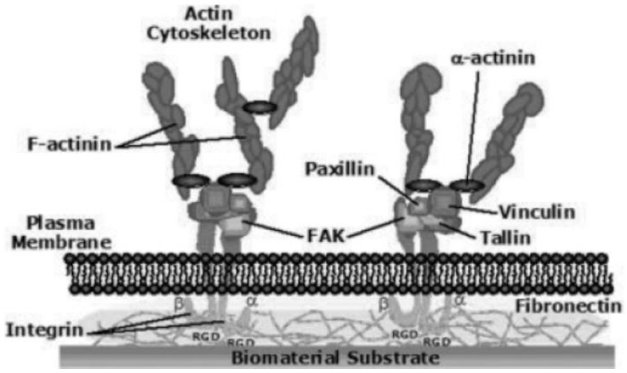

Figure 2.6 Schematic representation of cell or surface interaction of cell adhesion to a biomaterial substrate: adapted (Chen et al, 2006).

2.9 Nanoparticles for Drug Delivery

2.9.1 Magnetic nanoparticles

There are attractive properties driven from magnetic nanoparticles which render them applicable in the biomedical field. Magnetite is the most magnetic among all naturally occurring minerals on earth (Richard, et al., 2002). Magnetite forms part of the spinel

group, with a standard formula of $A(B)_2O_4$ where the letters; A and B are, receptively different metal ions that occupies specific sites within the crystal structure. Within magnetite (Fe_3O_4), the letters A and B correspond to $Fe+^2$ and $Fe+^3$, respectively.

The arrangement of $Fe+^2$ and $Fe+^3$ (Gossuin et al., 2009) enables electron transfer between the different types of iron ions in the structure. This generates a magnetic field through an electric field vector.

Figure 2.4 illustrate the arrangement of Fe+2 and Fe+3 ions on the face centered cubic structure of magnetite. The iron ions are located within the tetrahedral and octahedral sites, surrounded by oxygen ions (Gossuin, et al., 2009).

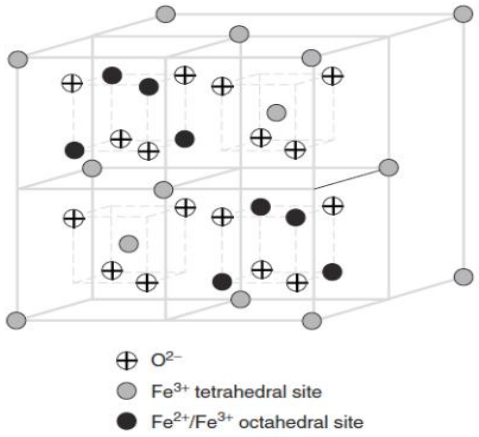

Figure 2.7 Iron Oxide crystal structure, Adapted from Gossuin et al., 2009. Magnetic Relaxation properties of superparamagnetic particles.

Maghemite nanoparticles have also been explored in hyperthermia treatment of tumors under a magnetic field (Ruizhi et al., 2007).

3.9.2 Magnetic Nanoparticles Heating

Hyperthermia treatment of cancer tumor can be induced in the tissue by generating heat due to an alternating magnetic field within a region in which magnetic materials are implanted. The small magnetic nanoparticles within the tissue can induce heating due to

hysteresis losses (Spiers et al., 2004). Hyperthermia treatment requires a magnetic material with the best heat evolution. In prior work (Akkaya, 2011) alternating magnetic fields have been used to induce hyperthermia around a Bio-Micro-Electro-Mechanical-Systems (BioMEMS) that were designed to induce both heat diffusion and drug diffusion. The heating was associated with the magnetic nanoparticles that were embedded in the polydimethyl siloxane (PDMS) and the fluid within PNIPA-based gels.

It is important to relate the energy dissipation of magnetic fluid to the first law of thermodynamics. This gives:

$$dU = dW + \delta Q \tag{2.4}$$

where U is the internal energy, W is the magnetic work done on the BioMEMS (system) and, Q is the heat added to the system. Therefore, the magnetic work can be estimated from the internal energy for an adiabatic process (Q= 0). This is given by:

$$\Delta U = -\mu_o \int M dH \tag{2.5}$$

where M is the magnetization, H is the magnetic field intensity and μ_o is the permeability of free space (Frisch, 1980). The resulting heat can diffuse through the tissue and the BioMEMS device to induce tumor shrinkage and cancer cell death via hyperthermia. Synergy can also be promoted by the combined use of heat and drug diffusion in the localized treatment of cancer (Oni and Soboyejo, 2010).

3.9.3Reference for chapter two

- Afrassiabi, A.S. Hoffman, L.A. Cadwell (1987), Journal of Membrane Science 33, pg191.
- Ala Alwan, (2011), World Health Organization, “Global Status Report on noncommunicable diseases in 2010”.
- Alberts B, Bray D, Lewis J, Raff M, Roberts K, Watson JD. Molecular Biology of the Cell, 3rd ed. New York: Garland;1995Anselme K. (2000) Osteoblast adhesion on biomaterials. Biomaterials; 21:667–681.
- Ali Montazeri (2008) Journal of experimental and clinitcal cancer research, Health-related quality of life in breast cancer patients, Iranian center for breast cancer and Iranian institute of Health Sciences Research.
- Anselme K. (2000) Osteoblast adhesion on biomaterials. Biomaterials;Vol. 21:pp667–681.
- Antunes F., Gentile L., Tavano L., Oliviero Rossi C., " Rheological characterization of the thermal gelation of poly(N-isopropylacrylamide) and poly(N-isopropylacrylamide)co-Acrylic Acid". Applied Rheology, 2009, Vol. 19, n. 4, pp. 42064-42069.
- Ashraf, M.W.; Tayyaba, S.; Afzulpurkar, N.; Nisar, A. Fabrication and analysis of tapered tip silicon microneedles for mems based drug delivery system. Sens. Transducer 2010, 122, 158–173.]
- Atala A., W. Kim, K.T. Paige, C.A. Vacanti, A.B. Retik (1994), The Journal of Urology 152, pp641 discussion 644.
- Bangham D., Standish M. M., Watkins J. C., Diffusion of univalent ions across the lamellae of swollen phospholipids, J. Mol. Biol. 813 (1965) 238-252.
- Bar, Y. H.; Okano, T.; Hsu, R.; Kim, S. W. (1987), Macromol Chem Rapid Commun,vol. 8, p48

- Bert Hildebrandt, Peter Wust, Olaf Ahlers, Annette Dieing, Geetha Sreenivasa, Thoralf Kerner, Roland Felix, Hanno Riess (2002), "The cellular and molecular basis of hyperthermia",Charite Medical School, Humboldt-Uni!ersity, Campus Virchow Clinic.
- Brizel D. M, M.E. Albers, S.R. Fisher, R.L. Scher, W. J. Richsmeier, V. Hars, Hyperfractioned irradiation with or without concurrent chemotherapy for locally advanced head.
- Brode, G. L. and Koleske, J. V. Lactone "Polymerization and properties, Journal of macromol. Science, A6," PP 1109-1144, 1972.
- Burd R, Dziedzic TS, Xu Y, Caliguiri MA, Subjeck JR, Repasky EA. (1998), "Tumor cell apoptosis, lymphocyte recruitment and tumor vascular changes are induced by low temperature, long-duration (fever-like) whole-body hyperthermia". J. Cell Physiol;177:137–47.
- Burridge K, Fath K, Kelly T, Nuckolls G, Turner C. (1988) Focal adhesions: Transmembrane junctions between the extracellular matrix and the cytoskeleton. Annual Review Cell Biol;Vol. 4:pp487–525.
- Brizel D. M, Albers M.E., Fisher S.R., Scher R.L., Richsmeier W. J., Hars V., Hyperfractioned irradiation with or without concurrent chemotherapy for locally advanced head.
- Cancer incidence and mortality worldwide: Lyon, International Agency for Research on Cancer, 2011 (IARC Cancer Base No.10).
- Chaplin D. J., S. A. Hill, K. M. Bell, G. M. Toser, Modication of tumor blood flow: Current states and future directions, semin.Radiat. Oncol. 8 (3) (1998) 151-163.
- Chen J., S. Mwenifumbo, Langhammer C., McGovern J.P., M. Li, A. Beye,. Soboyejo W. O (2006), "Cell/Surface Interactions and Adhesion on Ti-6Al-4V: Effects of Surface Texture

- Chung, J. E.; Yokoyama, M.; Yamato, M.; Aoyagi, T.; Sakurai, Y.; Okano, T. "Thermo-responsive drug delivery from polymeric micelles constructed using block copolymers of poly(N-isopropylacrylamide) and poly(butylmethacrylate)" Journal of Controlled Release, 1999, Vol. 62, pp115–127
- Cicek, H.; Tuncel, A (1998). J Polym Sci A Polym Chem, 36, 527.
- Cutierrez David, (2008), America Cancer Society, "Cancer facts and figures, 2nd edition.
- Chaplin D. J., Hill S. A.,. Bell K. M, Toser G. M., Modication of tumor blood flow: Current states and future directions, semin.Radiat. Oncol. 8 (3) (1998) 151-163.
- David Needhama, Mark W. Dewhirst (2001), "The development and testing of a new temperature-sensitive drug delivery system for the treatment of solid tumors" ELSEVIER Department of Mechanical Engineering and Materials Science, Duke University , Department of Radiation Oncology, Duke University Medical Center, , Advanced Drug Delivery Reviews 53, pp285–305.
- De Las Heras Alarcon, Pennadam S., Alexander C. (2005), Chemical Society Reviews 34, pg276.
- Dewey WC. (1994), "Arrhenius relationships from the molecule and cell to the clinic". Int J Hyperthermia;10(4):457–83.
- Dewhirst MW, Prosnitz L, Thrall D, et al. (1997), "Hyperthermic treatment of malignant disease: current status and a view toward the future". Sem Oncol;24(6):616–25.
- Dumbleton JH, Manley MT, Edidin AA (2002). A literature review of the association between wear rate and osteolysis in total hip arthroplasty. J Arthroplasty;15:pp649–661.
- Farmer T. G., Edgar T. F., Peppas N. A., Industrial and Engineering Chemistry Research 47 (2008), 10053.

- Feng B, Weng J, Yang BC, Chen JY, Zhao JZ, He L, Qi SK, Zhang XD. Surface characterization of titanium and adsorption of bovine serum album. Mater Charact 2003;49:129–137.
- Ferlay J et al. Estimates of worldwide burden of cancer in 2008: GLOBOCAN 2008. International Journal of Cancer, 2010, 127:2893–2917.
- FLORY P., in "Principles of Polymer Chemistry" (Cornell University Press, 1953) pp. 470
- Frisch H L (1980), "Sorption and transport in glassy polymers", polymer Eng. Sci. 20, pp2-12.
- Fu G. and Soboyejo W. O. (2009), "Swelling and diffusion characteristics of modified poly (N-isopropylacrylamide) hydrogels", Materials science and engineering
- Gareth A. Hughes, (2005), "Nanostructure-mediated drug delivery", Nanomedicine: Nanotechnology, Biology, and Medicine 1 22– 30.
- Gossuin, Y. et al. Magnetic Relaxation properties of superparamagnetic particles, Wiley Interdisciplinary Reviews: Nanomedicine and Nanobiotechnology Volume 1, Issue 3, Article first published online: 11 MAR 2009.
- Haim I. Bicher (1980), "The physiological Effects of Hyperthermia, Radiation Biology.
- Hildebrandt B, Wust P, Rau B, Schlag PM, Riess H. (2000), "Regional hyperthermia in rectal cancer". Lancet;356(9231):771–772.
- Hildebrandt B, Wust P, Rau B, Schlag PM, Riess H. (2000), "Regional hyperthermia in rectal cancer". Lancet;356(9231):771–772.
- Hildebrandt B., P. Wust in: W.P. Ceelen (Ed), Peritoneal Carcinomatosis: A Multidisciplinary Approach, Springer, New York, 2007, p. 185.
- Hu Yan and Kaoru Tsujii. "Potential application of poly(N-isopropylacrylamide) gel containing polymeric micelles to drug delivery systems" Colloids and Surfaces B: Biointerfaces. 2005, 46, 142–146.
- Inc. J Appl Polym Sci 99: 37–44, Istanbul Technical University, Department of Chemistry, Maslak, 80626 Istanbul, Turkey

- Issels R, Prenninger SW, Nagele A, et al. (1990), "Ifosfamide plus etoposide combined with regional hyperthermia in patients with locally advanced sarcomas". J Clin Oncol;11:1818–29
- Jeong, A. Gutowska (2002), Trends in Biotechnology 20, pg 305.
- John M. Walker (1996) "The Protein Protocols Handbook", University of Hertfordshire, Hatfield in UK. Humana press Inc. pp55-56,63.
- Jondavid Pollock (2006), National Cancer Institute webside (http://www.cancer.gov) and The National Women's Health Information Centre website (http://www.4woman.gov).
- Kabra B. G. and Gehike S. H., Polym. Commun., pp32, pp322 (1991).
- Kaifeng Liu, Tomothy C. Ovaert, James J. Mason (2007) "Preparation and mechanical characteristics of a PNIPA hydrogel composite", University of Notre Dame, USA, Department of Aerospace and Mechanical Engineering.

- Kaifeng Liu, Tomothy C. Ovaert, James J. Mason (2007) "Preparation and mechanical characteristics of a PNIPA hydrogel composite", University of Notre Dame, USA, Department of Aerospace and Mechanical Engineering.

- Kaneko, Y.; Sakai, K.; Kikuchi, A.; Yoshida, R.; Sakurai, Y.; Okano, T (1995). Macromolecules, 28, 7717.
- Kee D. D. , Q. Liu and J. Hinestroza (2005), The Canadian Journal of Chem. Eng. 83: pp913-929,.
- Koleske, J. V. Blends containing poly(ϵ caprolactone) and related polymers, in polymer Blends, Vol. 2 (R. Paul and S. Newman, eds), Academic press, New York,
- Lauffenberger DA, Horwitz AF. (1996) Cell migration: A physically integrated molecular process. Cell;84:pp359–369.
- Mark Chasin and Robert Langer (1990), Biodegradable polymers as drug delivery systems, p231.

- Melissa Center, Rebecca Siegel, Ahmedin Jemal, GLOBACAN 2008, American Cancer Society, Global Cancer facts and figure, 2nd Edition, World Health Organization, 2008. Estimated number of new cancer cases by world area, 2008.
- Oh, K. S.; Oh, J. S.; Choi, H. S.; Bae, Y. C. (1998), Macromolecules, 31, pp7328.
- Okay, O. (2000), Prog Polym Sci, 25, pp711.
- Oleson JR, Samulski TV, Leopold KA, et al. (1993), "Sensitivity of hyperthermia trial outcomes to temperature and time: implications for thermal goals of treatment". Int J Radiat Oncol Bio Phys;25 (2):289–97.
- Oni Y., C. Theriault, Hoek A. V., Soboyejo W. O. (2010), "Effects of temperature on diffusion from PNIPA-Based gels in BioMEMS device for localized chemotherapy and hyperthania", Journal of Materials science and Engineering C.
- Oyku Akkaya (2011), "An implantable Biomedical Device for localized hyperthermia and drug delivery", Thesis in the Department of mechanical and Aerospace Engineering, Princeton University.
- Park T.G. (1999), Biomaterials 20, p517.
- Pelton R.H., P. Chibante (1986), Colloids and Surfaces 20 247.
- Peppas N. A. (1987), "Hydrogels in medicine and pharmacy", CRC Press, Boca Ratons, FL.
- R. Hergt, R., Hiergeist, I. Hilger, W. A. Kaiser, Y. Lapatuikov, S. Margel and U. Richter (2004), 'Maghemite nanoparticles with very high AC- losses for application in RF-magnetic hyperthermia', Elsevier journal of magnetism and magnetic materials, vol 270. Abstruct.
- R.V. Kulkarni, B. Sa (2009), Journal of Biomaterials Science. Polymer ed. 20, p 235.
- R.V. Kulkarni, B. Sa (2009), Journal of Biomaterials Science. Polymer ed. 20, p 235.
- Rau B, Wust P, Tilly W, et al. (2000), "Preoperative radiochemotherapy in locally advanced or recurrent rectal cancer: regional radiofrequency hyperthermia correlates with clinical parameters". Int J Radiat Oncol Biol Phys;48(2):381–91.
- Richard J. Harrison, Rafel E. Dunin-Borkowski and Andrew Putuis (2002), 'Direct imaging of nanoscale magnetic interaction in minerals'.
- Ruizhi Xu, Yu Zhang, Ming Ma, et al., (2007), IEEE, vol. 43, 3, pg 1078-1085. Abstruct.

- Santini, J.T. Jr., Cima, M.J. & Langer, R. A controlled-release microchip. Nature 397, pp335–338 (1999).
- Schild H. G., "Progress in Polymer Science 17", (1992), p163. Institute of Macromolecular Chemistry, Academy of Sciences of the Czech Republic
- Schild H.G. (1992), Progress in Polymer Science 17, pg 163
- Schild, H. G. "Poly(N-isopropylacrylamide): experiment, theory and application" Progress in Polymer Science, 1992, 17 (2), 163–249.
- Schmaljohann D. (2006), Advanced Drug Delivery Reviews 58, 1655.
- Siepmann J. and Peppas N., (2001) "Modeling of drug release from delivery systems.
- Soppimath K.S., T.M. Aminabhavi, A.M. Dave, S.G. Kumbar, W.E. Rudzinski (2002), Drug Development and Industrial Pharmacy 28, pg 957.63
- Takata, S.; Suzuki, K.; Norisuye, T.; Shibayama (2002), M. Polymer 43, p3101.
- Tanaka, T.; Fillmore, D. J. J Chem Phys 1979, 70, 1214.
- Urano M, Kuroda M, Nishimura Y. (1999), "For the clinical application of themochemotherapy given at mild temperatures". Int J Hyperthermia;15:79–107.
- Willert HG, Buchhorn GH. The biology of the loosening of hip implants. In: Jakob RP, Fulford P, Horan F, editors. European Instructional Course Lectures, Vol 4. London: The British Editorial Society of Bone and Joint Surgery; 1999. pp 58–82.
- Wust P, Gellermann J, Rau B, et al. (1996), "Hyperthermia in the multimodal therapy of advanced rectal carcinomas". Recent Rec Cancer Res;142:281–309.
- Wust P, Stahl H, Dieckmann K, et al. (1996), "Local hyperthermia of N2/N3 cervical lymphnode metastases: correlation of technical/thermal parameters and response". Int J Radiat Oncol Biol Phys;34:635–46.
- Yong Qiu, Kinam Park (2001), "Environment-sensitive hydrogels for drug delivery", Departments of Pharmaceutics and Biomedical Engineering, Purdue University, West Lafayette, IN 47907-1336, USA, Advanced Drug Delivery Reviews 53 (2001) 321–339.
- Yoo M.K., Y.K. Sung, Y.M. Lee, C.S. Cho (2000), Polymer 41, pg 5713.

- Yoshida, R.; Uchida, K.; Kaneko, Y.; Sakai, K.; Kikuchi, A.; Sakurai, Y.; Okano, T. (1995) Nature, 374, 240.
- Yual Dogu, Oguz Okay (2005), "Swelling–Deswelling Kinetics of Poly(Nisopropylacrylamide) Hydrogels Formed in PEG Solutions", Wiley InterScienceInc. Journal of Applied Polymer Science 99: pp37–44.
- Zhang G. Q., Zha L. S., Zhou M. H., Ma J. H., Liang B. R., (2005), "Colloid and polymer science", Vol 283 p331.
- Zhang X.; Yang, Y.; Chung, T.; Ma, K. Langmuir 2001, 17, 6094.
- Zhang, J.; Cheng, S.; Huang, S.; Zhuo, R., (2003) Macromol Rapid Commun, 24, p447.
- Zhuo, R.; Li, W. (2003), Journal of Polymer Science, A Polym Chem 41, p152.

CHAPTER THREE

3.0 MATERIALS AND METHODS

3.1 Introduction

The chapter presents the experimental procedures that were used for: the fabrication of Poly(dimethylsiloxane) (PDMS) packages; the preparation of Poly(N-Isopropylacrylamide) (PNIPA)-based copolymers; the insertion of PNIPA base gels into PDMS packages, and fluid flow from the PDMS packages. The potential effects of temperature are also explored on the release of fluids and cancer drugs from thermosensitive PNIPA gels and their comonmers.

This study explores the effects of temperature on the diffusion of cancer drugs. The drug release kinetics of the gels are elucidated between temperatures of 37- 48˚C.

3.2 Apparatus

The apparatus that were used in the PNIPA gel synthesis include: a water bath, thin cylindrical rods with blunt ends, a parafilm, waterproof tape, pipettes (2µl, 10µl, 20µl and 100µl), as shown in Figure 3.1A.

The materials that were used in the PNIPA gel synthesis (Figure 3.1B and Table 3.1) were purchased from Sigma Aldrich Co., St. Louis, MO in the USA. They were used directly in the powdered form in the as-received condition.

A B

Dimension: 369x252 pixels 100mm Dimension: 477x252 pixels 100mm

Figure 3.1A Apparatus used in PNIPA-based gel preparation; Figure 3.1B Chemicals used in the PNIPA-based gel preparation.

Table 2Table 3.1 Gel materials and their role in gel polymerization

Gel materials and their reagent grade	**Function**
N-Isopropylacrylamide (NIPA), 97 %	Monomer
N,N,N',N'-tetra-methyl-ethylene-diamine (TEMED), 99 %	Cross-linkers used in conjunction with APS to accelerate the rate of acrylamide polymerization
N,N'-methylene-bis-acrylamide (MBA), 99 %	Cross-linking agent
Ammonium persulfate (APS), 98 %	Used as radical Initiator
Acrylamide (AM), 99.9 %	Hydrophilic Compound

3.3 Experimental Procedures

3.3.1 Preparation of PNIPA-Based Hydrogels

The gels were prepared by free radical polymerization (Tanaka, 1981; Zumdahl, 2005). Acrylamide (AM) comonmers were co-polymerized with PNIPA, as summarized in Table 3.2. The ratios of NIPA, MBA and AM were in accordance with prior work (Oni et al, 2011).

Initially, PNIPA gels were first prepared by weighing 0.7776 g of PNIPA, 0.01219 g of MBA, 0.02997 g of APS with an analytical weighing balance (Ohaus Analytical Plus). This was done inside a fume hood as shown in Figure 3.2A.

The weighed samples were introduced into 24 ml falcon tubes that were subsequently topped up with 7 ml distilled water. The solution was prepared by stirring vigorously until all the PNIPA was dissolved at 24 ^{o}C to produce homogenous solutions. The falcon tubes containing the solutions were then placed in a beaker containing 1000g of ice, and then sonicated, while Nitrogen gas was bubbled through the solution for 20 minutes at 10 bars to remove all of the dissolved oxygen (Figure 3.2B).

Subsequently, 40 µl of TEMED was pipetted rapidly into the solution to prevent oxygen uptake, since the reactions are enhanced by free radicals. The mixture was then stirred vigorously, while the TEMED initiated the gelation process after about five minutes. The solution was poured into smaller cylindrical molds with diameters of 0.8 and 1 cm (Figure 3.3A).They were then exposed to the lab environment (standard temperature and pressure) to terminate the free radical polymerization.

The samples were left at 25˚C (in a water bath) to complete the polymerization process for 6 hours. Some gels were left without APS and TEMED for over 24 hours. No gelation was observed in these samples, thus confirming the role of the initiators.

PNIPA copolymers were also prepared by mixing PNIPA with acrylamide (AM). The mixtures were then copolymerized using procedures summarized in Table 3.2 below. The AM was used to change the critical transition temperatures of PNIPA-based gels.

Table 3.2 shows the PNIPA and PNIPA gel composites percentages

Gel Cod	Gel composite
A	PNIPA (100 %)
B	PNIPA-co-Am (95-5%)
C	PNIPA-co-Am (90-10%)
D	PNIPA-co-Am (85-15%)

A 

Dimension: 474x310 pixels 100mm

B 

Dimension: 415x310 pixels 100mm

Figure 3.2A shows the weighing of samples inside a fume hood; Figure 3.2B Shows the de-gassing set up with nitrogen gas at 10 bar.

After the polymerization process, the gels were carefully removed from the cylindrical molds (Figure 3.3B). They were then washed with deionized water, and subsequently cut into discs and cylindrical shapes (Figure 3.3C).

A 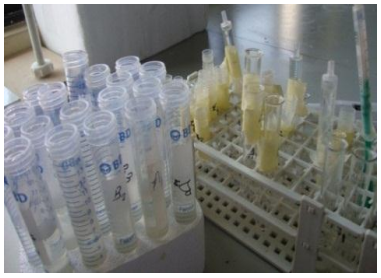 B 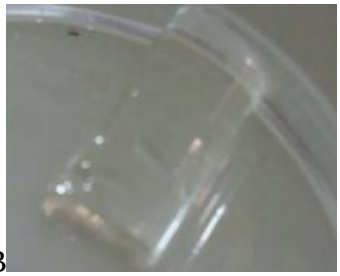 C 

Figure 3.3A Gel solutions inside smaller tubes, Figure 3.3B Transparent cylindrical gel removed from the mold placed in a Petri-dish, and Figure 3.3C Disc of gels cut with a razor blade into smaller cylinders with thicknesses ~ 3mm.

The hydrogels were washed several times with dionized water to remove chemical residue. They were then soaked in distilled water for a week, while the water was changed on a daily basis. This enhanced the chances of removing any form of an unreacted chemical. It also allowed the gels to swell to equilibrium. The gels were then dried in an oven at 45 ˚C for 24 hours.

This present work, EVO^{R} analytical scanning electron microscope (SEM) series (Oxford Intrument, MA10) was used to further explore the inner structure of both conventional PNIPA and PNIPA copolymers with an accelerating voltage of 20kV.

3.2.2 Poly (Di-methyl-Siloxane) (PDMS) Replication

PDMS packages with different channel lengths and reservoir sizes were obtained according to the standard sylgard preparation guide (sylgard 184kit, Dow corning, MI) (Peppas and Wright, 1998). The PDMS was prepared by mixing the sylgard to a silicon elastomer curing agent in a 10:1 ratio by volume. The mixture was stirred vigorously, de-gassed with a GALVAC vacuum oven (LTE Scientific LTD., Greenfield) at -18 in Hg with no heat for 1hour, and 15 minutes. This was done to provide enough time for the removal of bubble or entrapped gases (Figure 3.5A).

The de-gassed PDMS was then poured into cubic Aluminum molds (Figure 3.5B). Some of the PDMS was also poured into cylindrical molds with integrated micro-channels (Figure 3.5b) that were designed to enable flow from the reservoirs or gels. De-gassing was done again after pouring the PDMS into the molds (under a vacuum at ~ -18 in Hg) to remove entrapped bubbles or gases. The samples were then left to cure at either 28 ˚C for 48 hours, or 60˚C for 3 hours, before removing them from the mold Table 3.3 summarizes the devices that were produced along with the different channel lengths.

A  **B**  **C**  **D** 

Figure 3.5a shows de-gassing of PDMS in a weighing boat, (b) different sized of Al molds loaded with PDMS, c shows different sizes of PDMS produced, and d is showing the micro-channels produced in the cylindrical mold.

Table 3Table 3.3 Devices and their channel lengths

Device	Side length (cm)	Height (cm)	Channel length (cm)	Reservoir height (cm)
1	1.6	0.8	0.5	0.54
2	1.95	1.21	0.7	0.90
3	2.3	2.	0.7	1.7
4	1.2	1.2	0.2	0.8
5	1.45	1.48	0.55	0.43

3.3.3 Encapsulation of PNIPA in PDMS Packages

PNIPA gels were soaked to saturation (Figure 3.6A) in a dye (bromophenol blue) or prodigiosin (a cancer drug) (Williamson et al., 2006; Williamson et al., 2007) in Figure 3.6B for 5 days.

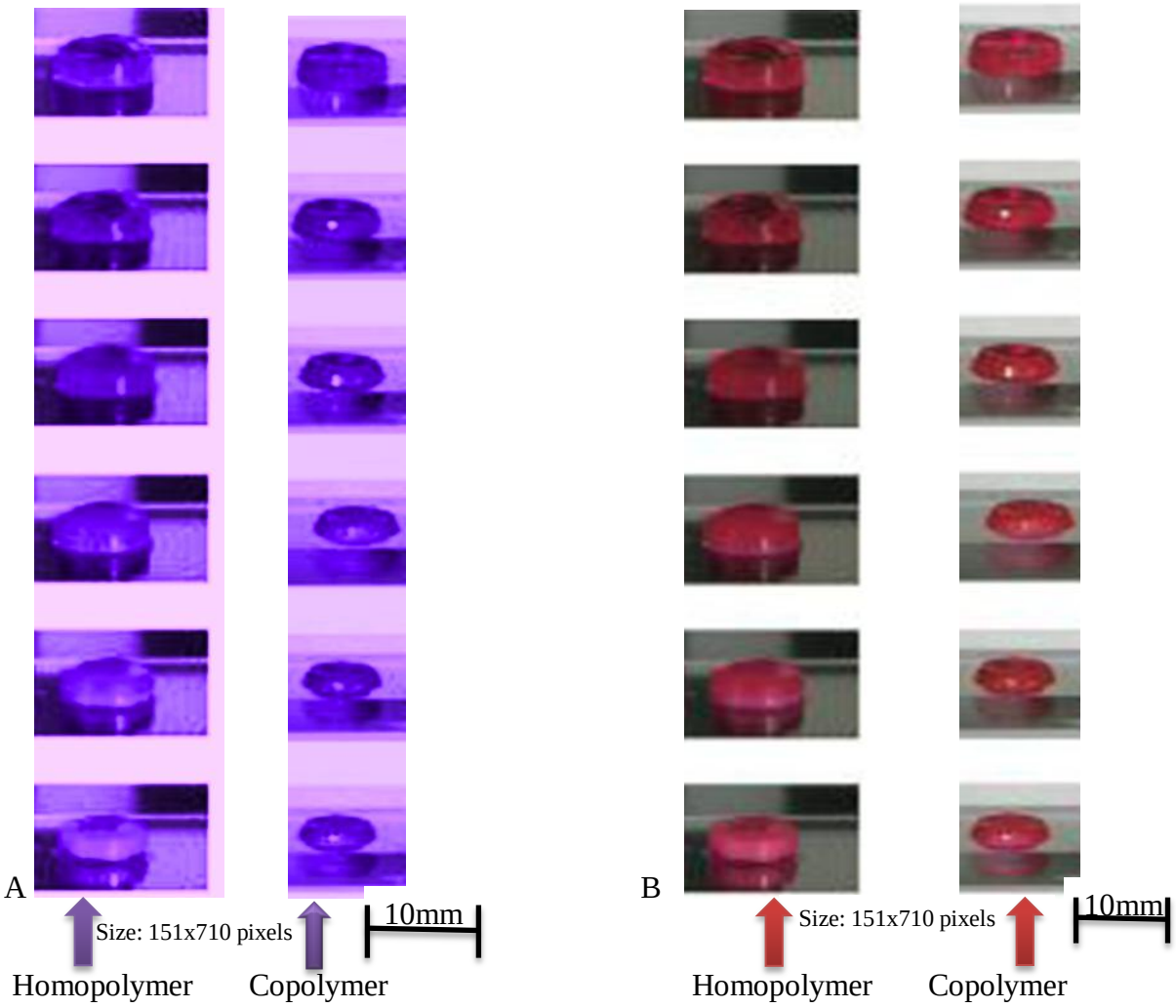

Figure 3.6A PNIPA gels soaked to saturation in a dye; Figure 3.6B PNIPA gels soaked to saturation in prodigiosin

They were inserted into the PDMS reservoirs (Figure 3.7A). The reservoir was closed with a PDMS cover by applying a curing agent on both edges. The two layers were properly sealed by applying a slight pressure with a clamping device on the axes perpendicular to the edges (Figure 3.7C-D) and allowed at 28˚C for 24 hours to complete the polymerization of the two layers. A syringe was used to introduce more bromophenol blue, and prodigiosin into the PNIPA encapsulated in a slightly manner.

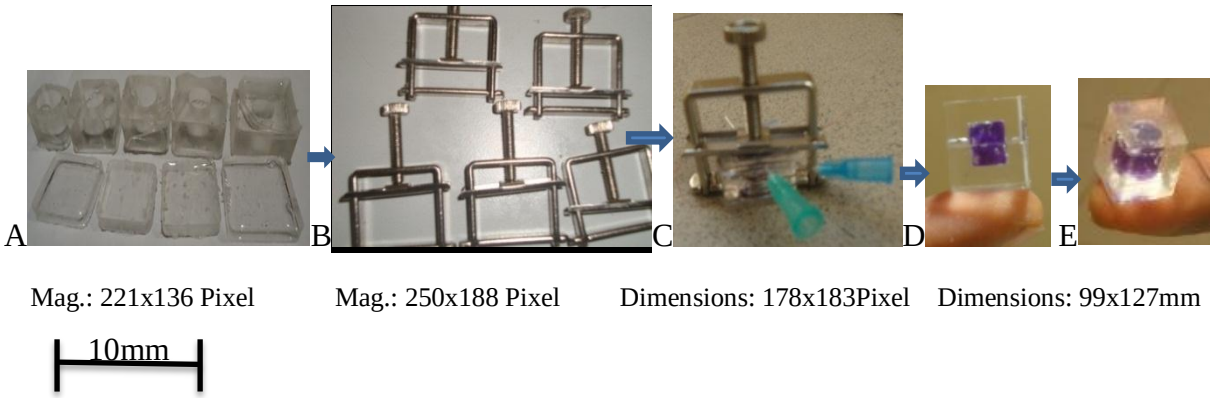

Figure 3.7; (A) PDMS packages: (B) Clamping devices; (C) Clamped encapsulated device with surgery needles used to create micro-channels within the device; (D) Encapsulated PNIPA in a PDMS package; (E) Three-dimensional view of the device.

3.3.4 Drug Diffusion

Other devices were fabricated with 20 turns of copper wires worn around an insulator. PNIPA was encapsulated in them, and the devices were subjected to resistance heating at (45˚C).

The time for the fluid to flow across the devices with different channel lengths was measured by recording the time taken by the first droplet to reach the edge of the device. This was done to ascertain the diffusion coefficient, D (i.e. flow of fluid) across the channel length, L. The diffusion coefficient, D was obtained from:

$$L = \sqrt{Dt} \tag{3.3}$$

where D is the effective coefficient of diffusion through the channel length (L), t is the time taken to diffuse across L.

The experimental setup for the diffusion of bromophenol blue or prodigiosin is shown below in Figure 3.8A. The diffusion of bromophenol blue across the channel length (with thermocouples to record the temperatures at intervals of 2.5 cm away from the BioMEMS

device) is shown (Figure 3.8B-C). This was to study the release of fluid or drugs at temperatures close to hyperthermic regime.

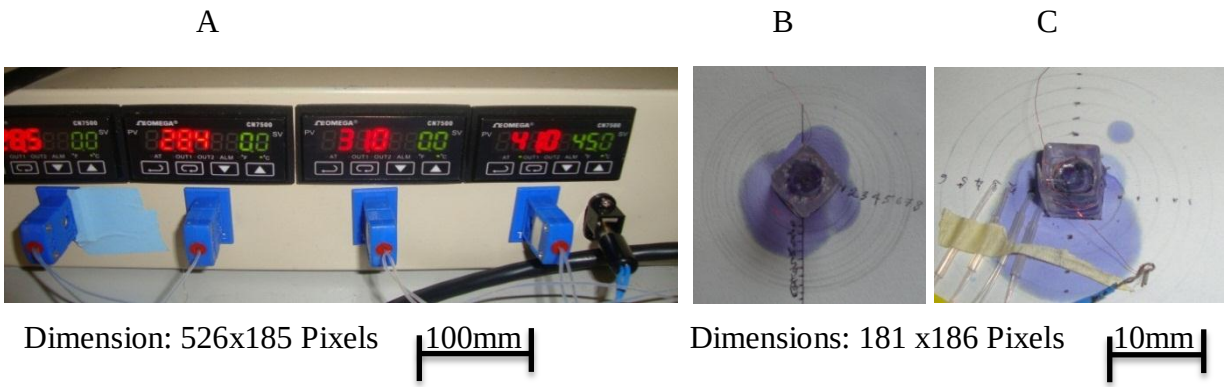

Figure 3.8 Setup for the hyperthermia of bromophenol blue released across the channel length. The temperature gradient was radially distributed across the device when it was heated at 45˚C.

3.4 Fluid Release from PNIPA-Base gels

Bromophenol blue solution was prepared by dissolving 0.1g of Bromophenol blue powder in a 100 ml of 20 % ethanol, and topped-up with 100 ml of distilled water. The color change from yellow to blue-violet and the pH varied from 3.0-4.6. The gel release kinetics were characterized by soaking samples of dried gels in bromophenol blue, water, and prodigiosin an anticancer drug (Williamson et al., 2006; Williamson et al., 2007) to saturation at temperatures (28˚- 48˚C) for 4 days. This was done to provide enough absorption time for the fluids. Some gels were loaded with an equal concentration of bromophenol blue and then allowed to swell to equilibrium at 37˚C.

3.5 UV-VIS spectrometer

UV-VIS spectrometer (CECIL 7500) was used to obtain the absorbance and wavelengths for the dye and prodigiosin. The loaded gels were put into glass test tubes containing equal

volumes of distilled water (2.5 ml) at 37˚C. The absorbance of bromophenol blue together with prodigiosin were determined at equal time intervals of 5 minutes at 589 nm (Figure 4.8a), and 538 nm (Figure 4.8b), respectively. From Beer-Lambert law, it was possible to determine the concentration, absorbance and molar absorptivity relating to the UV-Visible adsorption spectrographs obtained for the bromophenol blue and the prodigiosin.

The concentration C, was obtained by:

$$C = \frac{(m/M)}{V} \tag{3.2}$$

where m is the mass of the dye, M is the molar mass of dye and V is the volume of distilled water.

In the current work, the mass of the powdered dye was 0.1 g, while the molar mass of dye was 669.96 g/mol. Since $1dm^3$ is equivalent to 100 ml, the volume of water used was 100 ml. Substituting these parameters into Equation (4.1) gives a dye concentration $7.46313x10^{-4}$ mol/dm^{-3}.

The molar coefficient of absorptivity of bromophenol blue was obtained using the concentration of dye at wavelength of 589 nm. The maximum peak absorbance was obtained from:

$$\varepsilon = \frac{A}{LC} \tag{3.3}$$

where A is the absorbance of bromophenol blue (0.911), L is the path length of the quartz cell used (1 cm), and C is the concentration of the dye. The molar absorptivity for bromophenol

blue was thus obtained to be 1220.67 dm^3/mol. Plots of absorbance versus wavelength (nm) were obtained, as shown (Figure 3.9a-b).

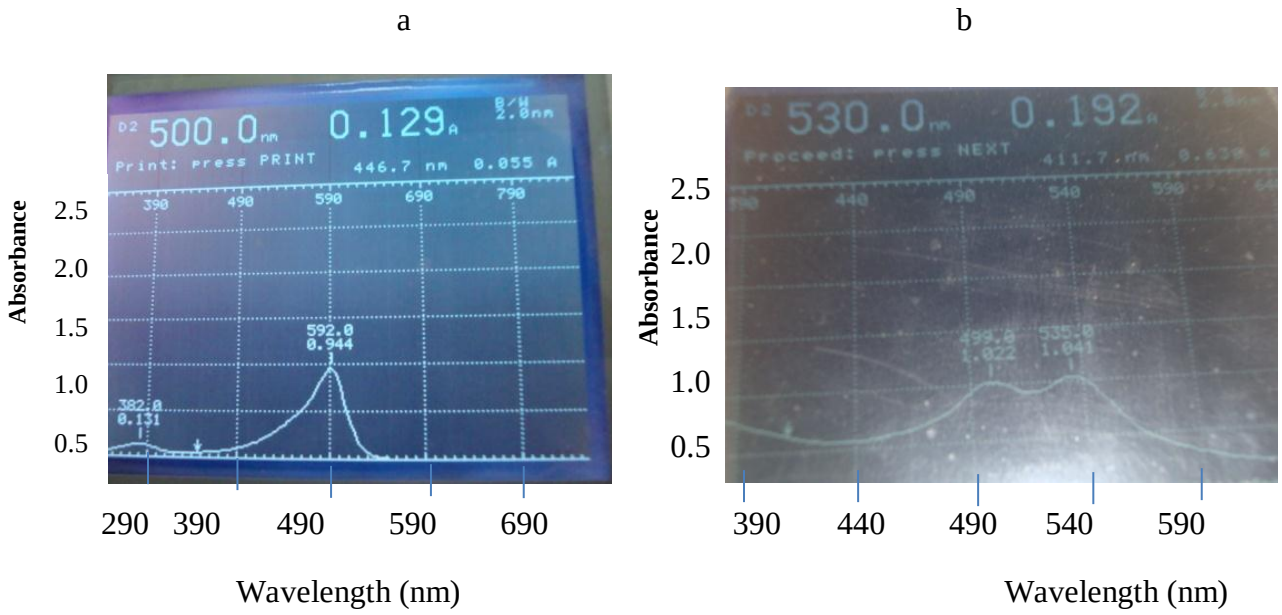

Figure 3.9 Plot of Absorbance Versus Wavelength (nm) Obtained from; (a) Bromophenol Blue, and (b) prodigiosin.

The initial bromophenol blue had a peak absorbance of 0.911 at a wavelength of 590 nm, while the prodigiosin had a peak absorbance of 0.488 at 535nm.

3.6 Diffusion and Swelling Kinetics

3.6.1 Kinetics of Bromophenol Blue

Samples A, B, C, D were selected to study the diffusion and swelling kinetics of PNIPA (denoted by A) and PNIPA gel composites (B, C, and D). Bromophenol blue solution was used for the diffusion measurements. The release percentage of the gels were normalized by m_t/m_∞ where m_t and m_∞ are the quantity of blue eluted from the gels at time t, and after some infinite time, respectively. In a similar way, the swelling kinetics was carried out by

taken the ratios of the weight of water taken-in by the various gels at setting time intervals (i.e 30 minutes interval). The weights of the hydrogels were determined after the gels were placed in between two pieces of filter paper to remove the excess water on the gel surface. Water retention W_R was determined by

$$W_R = {}^{W_t}/_{W_o} \tag{3.4}$$

Where W_t is the weight of the water taken-in by each hydrogel at time t during swelling, and W_o is the weight of the dried gel. Absorption experiments were carried out at different temperatures using a water bath (Gesseschaft fur Labortechink, MBH, D300) that was used to vary the temperature from 28-48˚C. The water uptake in the gels was obtained with the relative gel mass. This gives (Yual and Oguz, 2005):

$$\mathrm{M_{rel}} = \frac{\mathrm{M_t}}{\mathrm{M_s}} \tag{3.5}$$

where M_t is the mass of the gel samples at any time, t, and M_s is the swollen mass at 28^{o}C.

3.7 References for chapter three

- Coughlan D.C., Quilty F.P., Corrigan O.I. ((2004), Journal of Control Release, 98, p97.
- Hedenqvist, Angelstok A., Edsberg L., Larsson P., Gedde.W., Polymer 37 (1996) 2887
- Matsuo E.S., Tanaka T., Phase Transitions, 46 (1994) 217.
- Oni Y., Theriault C., Hoek A.V., Soboyejo W.O. (2011), "Effects of temperature on diffusion from PNIPA-based gels in a BioMEMS device for localized chemotherapy and hyperthermia", Materials Science and Engineering C, pp67-76.
- Peppas N.A., Pharmaceutica Acta Helvetiae 60 (1985) 110.
- Siepmanna J., Peppas N.A. (2000), "Modeling of drug release from delivery systems based on hydroxypropyl methylcellulose (HPMC)", Advanced Drug Delivery Reviews 48 (2001) 139–157
- Tanaka T. (1981) Gels. Sci. Am. 244 124.
- Williamson NR, Fineran PC, Gristwood T, Chawrai SR, Leeper FJ, Salmon GP (2007). "Anticancer and immunosuprressive properties of bacterial prodiginines". Future Microbiol. 6 (6); pp605-618.
- Williamson NR, Fineran PC, Gristwood T, Leeper FJ, Salmon GP (2006). "The biosynthesis and regulation of bacterial prodiginines". Nature Reviews Microbiology 4(12), pp887-899.
- Yoshida, R.; Uchida, K.; Kaneko, Y.; Sakai, K.; Kikuchi, A.; Sakurai, Y.; Okano, T. Nature 1995, 374, 240.
- Yual Dogu, Oguz Okay (2005), "Swelling–Deswelling Kinetics of Poly(Nisopropylacrylamide) Hydrogels Formed in PEG Solutions", Wiley InterScienceInc. Journal of Applied Polymer Science 99: pp37–44.
- Zumdahl S.S., (2005), Chemical Principles, Houghton Mifflin Company, Boston.

CHAPTER FOUR

4.0 Results and Discussion

4.1 Introduction

This chapter presents the results and discussion. Following the introduction, the structures of the gels produced are presented using light microscopy and scanning electron microscopy images. The swelling and fluid or drug release characteristics of the gels are then discussed within the context of fluid or drug release kinetics. The diffusion of fluid or drug, through microchannels in the PDMS packages, is examined before discussing the implications of the current results for applications of hyperthermic drug delivery devices.

It was noticed that the hyperthermia was maintained at 41˚C for about 30 minutes though the device was internally heated at 45˚C.

A linear graph of the length (L/cm) versus $\sqrt{t}$ was obtained (Figure 4.1) where the slope is equal to the square root of the diffusion coefficient, D.

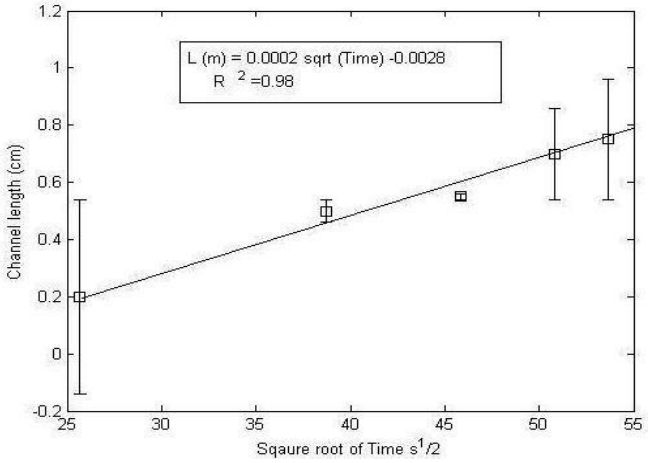

Figure 4.1 shows the plot of channel length versus square root of time for bromophenol blue release at 41˚C.

The equation of the straight line yielded a slope of $0.0001^{m}/_{S^{0.5}}$ from the graph (figure 3.5). The diffusion coefficient, D is obtained by taking square of the slope which gives us 1.0 x10^{-8} m^2/s.

4.2 Structure, Porosity and Surface Morphologies

Optical microscopy images of the PNIPA and PNIPA-AM copolymers are presented in Figures 4.2a-4.2b. The as-processed PNIPA gels contained pores with sizes between ~ 0.1microns and 0.7 microns (Figures 4.2c- 4.2d).

Further evidence of the microporous network within the gels was revealed by the bromophenol blue die, as shown in Figure 4.3a and 4.3b. The images also reveal evidence of the collapsed walls in the hydrogels (Figure 4.3c and d).

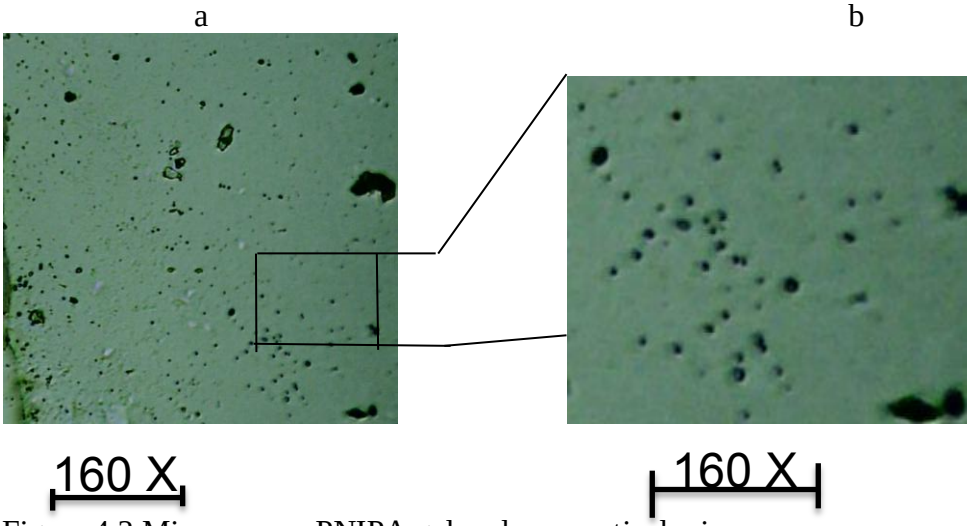

Figure 4.2 Microporous PNIPA gel under an optical microscope

c d

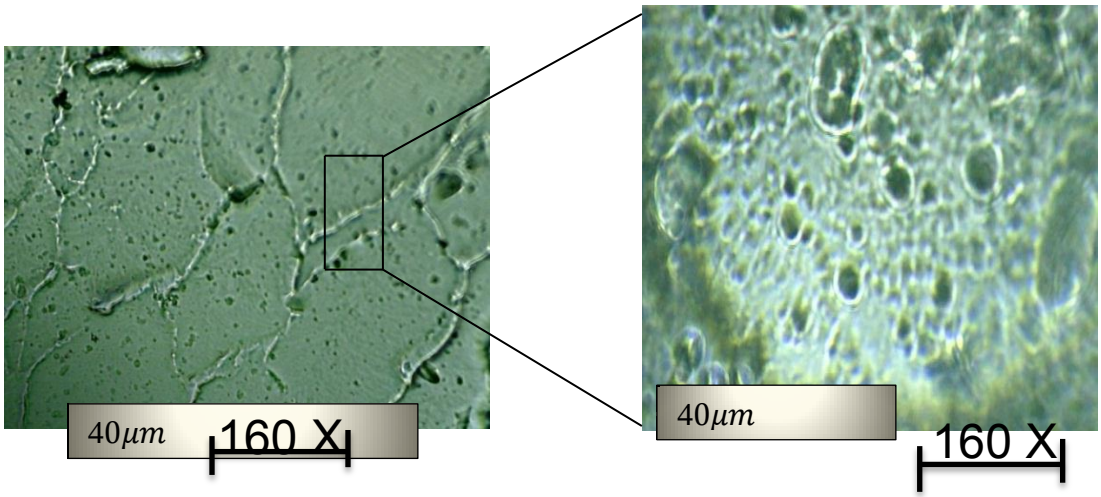

Figure 4.2. Light microscopy image of the PNIPA hydrogel soaked with a little diluted bromophenol blue showing clearly the micro-porous network, this has been magnified in the second image to the right.

a b

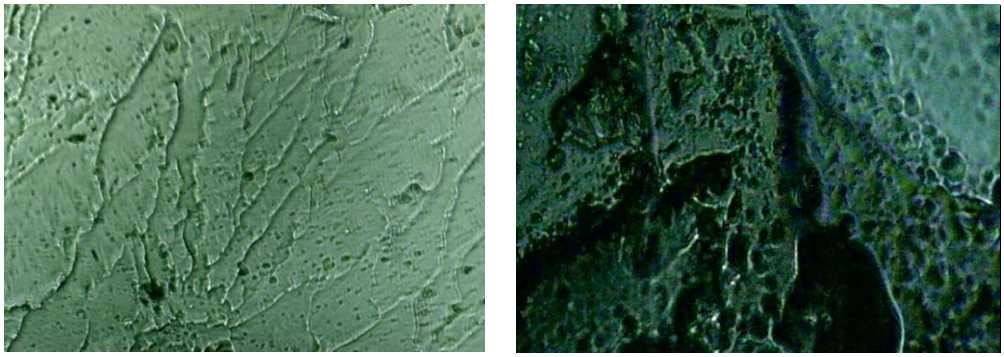

c d

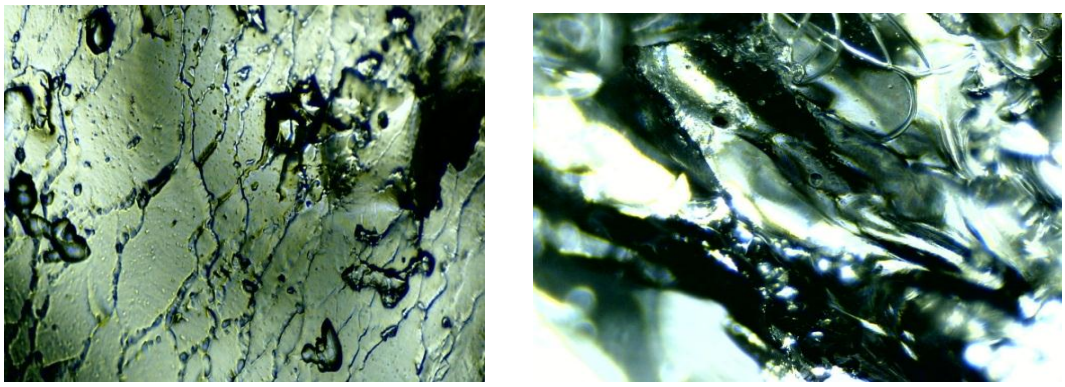

Figure 4.3 Light microscopy images of PNIPA hydrogel, soaked with a less diluted bromophenol blue showing clearly the micro-porous network. The gels also indicated the collapse wall of the gel in the dried state (Figure 4.2c,4.3).

This is consistent with the results from prior studies by Yoshida, (1995) that have shown dangling chain structures in PNIPA gels that can easily collapse and expand when an external stimulus is applied.

The SEM images provided higher magnification views of the porous structures, which were enhanced by the presence of prodigiosin (Figures 4.5a and 4.5b).

The SEM analysis revealed an increased in micro-porosity in order of the acrylamide copolymers (Figures 4.6a-4.6d). The acrylamide containing gels also contained second phase particles, as shown in (figures 4.6a-4.6d). Further work is needed to identify these second phase particles.

a b

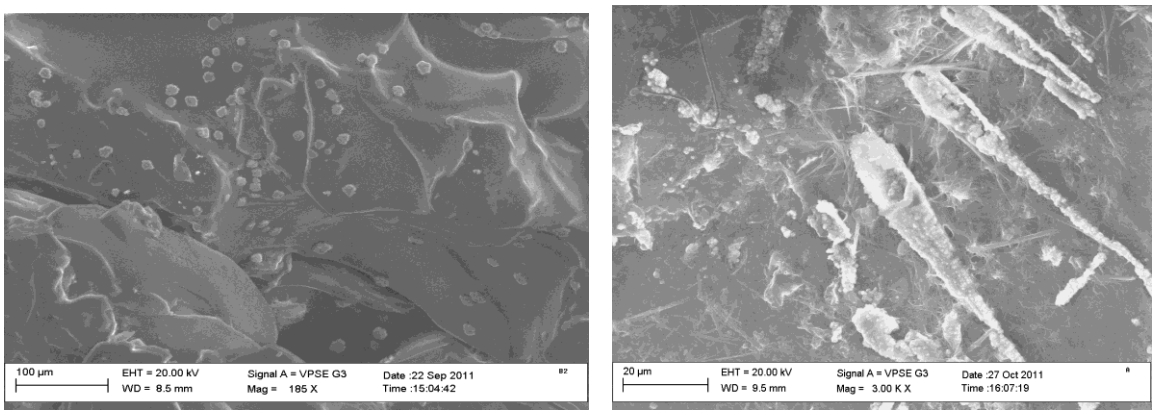

Figure 4.5 SEM image of PNIPA GEL, enhanced by the presence of prodigiosin

a b

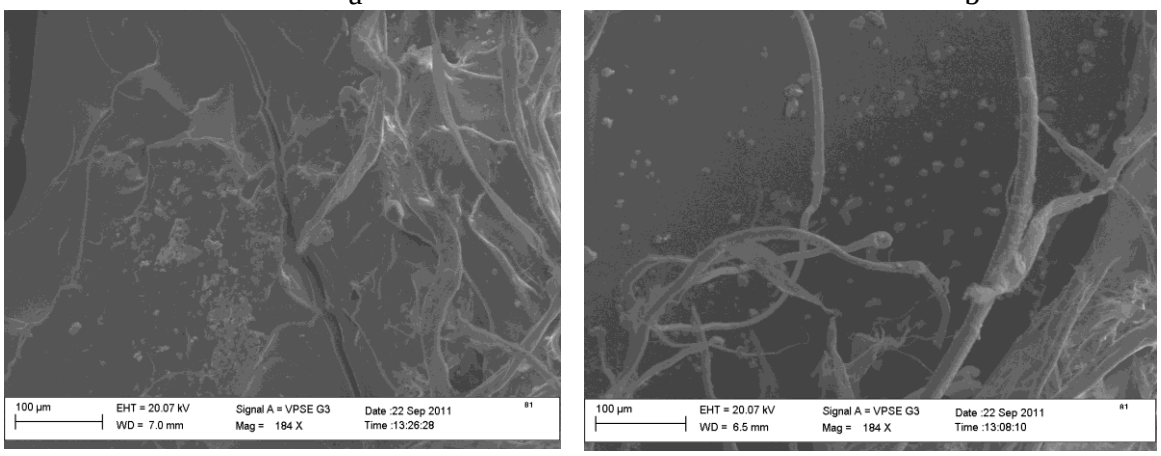

c **d**

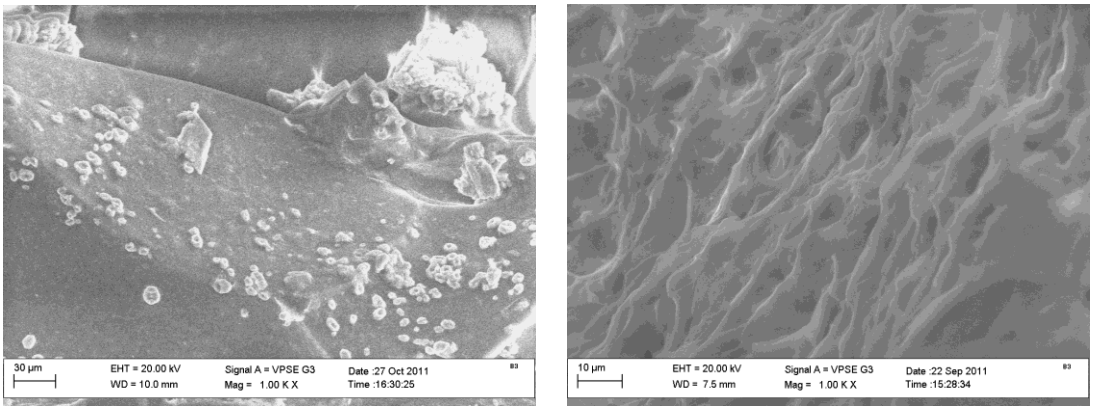

Figure 4.6 SEM image revealed an increased in micro-porosity in order of the acrylamide copolymers: (a) gel A; (b) gel B; (c) gel C, and (d) Gel D.

No evidence of porosity was observed in the PDMS structure, as shown in Figure 4.7 in which a typical SEM micrograph is presented. This shows clear evidence of smooth surfaces with some texture.

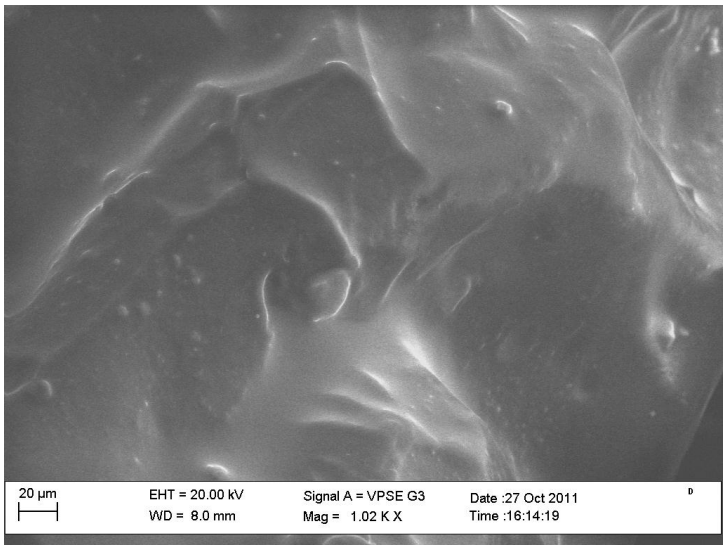

Figure 4.7 SEM image of PDMS

4.3 UV-VIS spectrometer

In the case of bromophenol blue, absorbance versus concentration is presented in Figure 4.9A-D for gels A- D. Each of the plots exhibited a linear dependence of absorbance on wavelength.

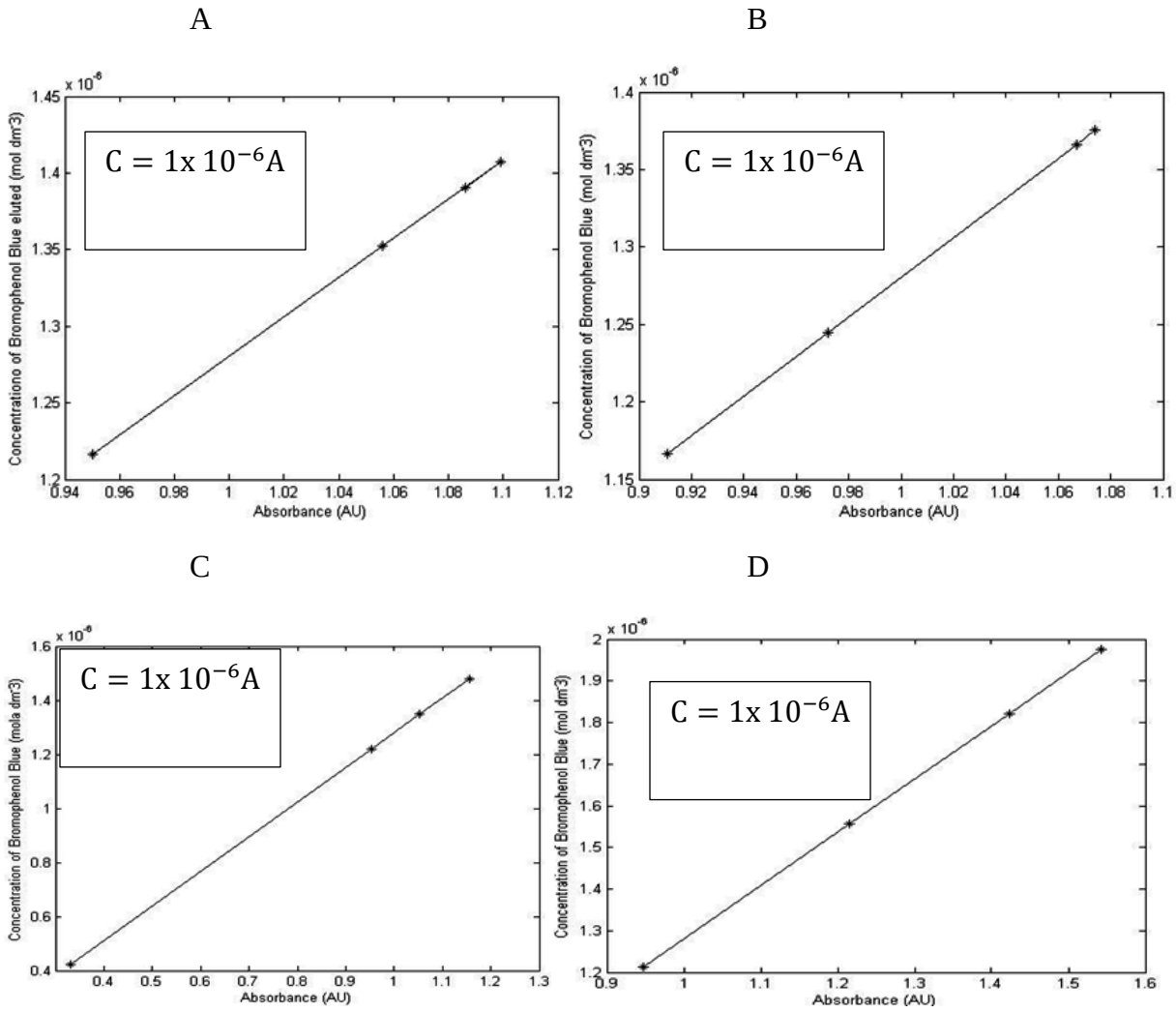

Figure 4.8 A Linear Plot of Concentration of Bromophenol Blue versus Absorbance for hydrogels; (A) Homopolymer; (B-D) Copolymers.

The diffusion coefficients were obtained from the concentration profiles using simple monolithic and membrane models (Heller et al., 2004; Baker et al., 1974). Regression coefficients, r^2, of 1 were obtained for each of the gels calibration curves.

The soaked gels with prodigiosin were immersed in a beaker containing warm distilled water. That was maintained at 37˚ to simulate body temperature). The concentrations were also increased at 5 minute intervals, after allowing the absorbance sufficient time to evolve to constant values at a given concentration. Similarly, in the case of the cancer drug, prodigiosin (Williamson et al., 2006; Williamson et al., 2007), linear plots of absorbance versus drug concentration were obtained from the plots of absorbance versus time (Figures 4.10a-d) for gels A-D.

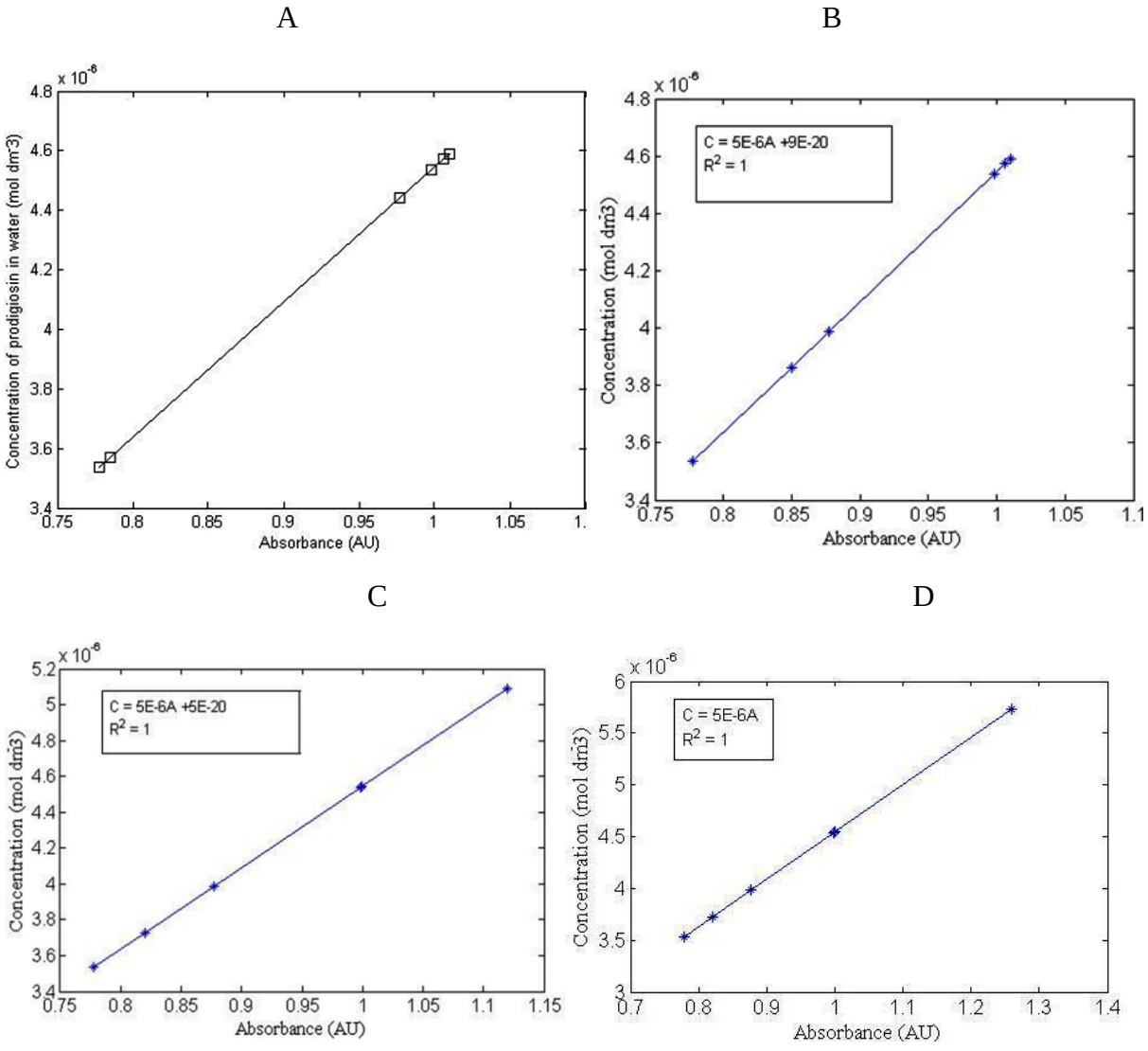

Figure 4.9 Linear Plot of Concentration of Prodigiosin versus Absorbance for hydrogels; (A) Homopolymer; (B-D) Copolymers.

4.4 Swelling Ratios

Figure 4.10 below shows the increase in size of gels from before and after swelling in distilled water.

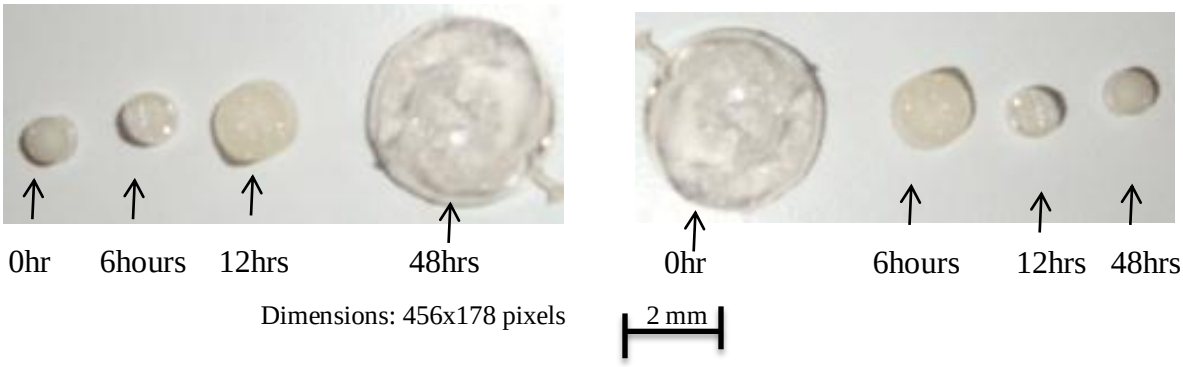

Figure 4.10 Swelling (A) and de-swelling (B) sizes of the hydrogel within 48 hours in distilled water at 28˚C.

The average swelling ratio (SR_A) was determined by soaking the PNIPA-based hydrogel in distilled water at regular time intervals of 30 minutes. This was continued until equilibrium mass was attained. The average swelling ratio was then obtained from:

$$SR_A = \frac{M_t - M_o}{M_o} \tag{4.1}$$

The swelling ratios obtained for the PNIPA-base gels are summarized in Table 4.1. This shows that the diameters increased by factors of ~ 1.5 for dye A to ~ 2.2 for dye D. It is important to note hear that the gels are capable of absorbing more water or fluid at lower temperatures (Oni and Soboyejo, 2011). Diffusion is alos more likely to occur in the amorphous areas of the matrix materials. The equilibrium swelling ratio, $SR_{eq.}$, was obtained from equation (4.2) (Coughlan et al., 2004): Thus

$$SR_{eq.} = \frac{M_{eq} - M_o}{M_o} \tag{4.2}$$

where M_t corresponds to the weights of the gel at time t, Mo is the mass of the dried gel at the initial time, and M_{eq} is the weight of the hydrogel at equilibrium. From the swelling

experiment at 28˚C, gel A finally saturated at M_{eq} of 1.1752g, M_{eq} for gel B was 1.2758g, M_{eq} for gel C was 1.4298g, and M_{eq} for gel D was 1.5422g prior to their dried weighs. The equilibrium swelling ratios obtained from equation 4.2 were 28.2 for gel A, 26.6 for gel B, 14.9 for gel C, and 24.0 for gel D. The equilibrium volume of the gels at the swollen state (V_{eq}) was determined from:

$$V_{eq} = \frac{D}{D_o} \tag{4.3}$$

where D_o and D are the diameters of the hydrogels, before and after the equilibrium swelling. The results obtained for the equilibrium volume are summarized in Table 4.1.

Table 4.1 Equilibrium volume for PNIPA-Based gels

Gel code	Do(mm)	D(mm)	D/Do
A (Homopolymer) 0 % AM	7.0	10.5	1.5
B (PNIPA-Co-AM) 5 %	6.5	11.0	1.7
C (PNIPA-Co-AM) 10 %	6.1	11.7	1.9
D (PNIPA-Co-AM) 15 %	5.5	12.0	2.2

Table 4.2 Swelling Ratios of the various PNIPA and PNIPA gel composites at 28˚C

Time (S)	swollen ratio A	Swollen ration B	swollen ratio C	swollen ratio D
0	0.00	0.00	00.00	0.00
9000	1.14	1.13	1.13	1.42
1800	1.27	1.49	1.72	2.00
3600	1.87	2.35	2.50	3.12
7200	2.64	3.44	3.66	4.80
10800	3.54	4.37	4.22	6.43

The swelling-induced changes in the gel sizes were quite remarkable, as shown in Figure 4.11a and b for swelling at 28 and 37˚C. The swelling ratios obtained at 41,43,45 and 48 are presented in Figure 4.11c-d. this shows that, the swelling ratios are of magnitude with respect to the acrylamide composition in the gel. However, swelling ratios are lower for gels at their critical transition temperatures (Oni, 2010).

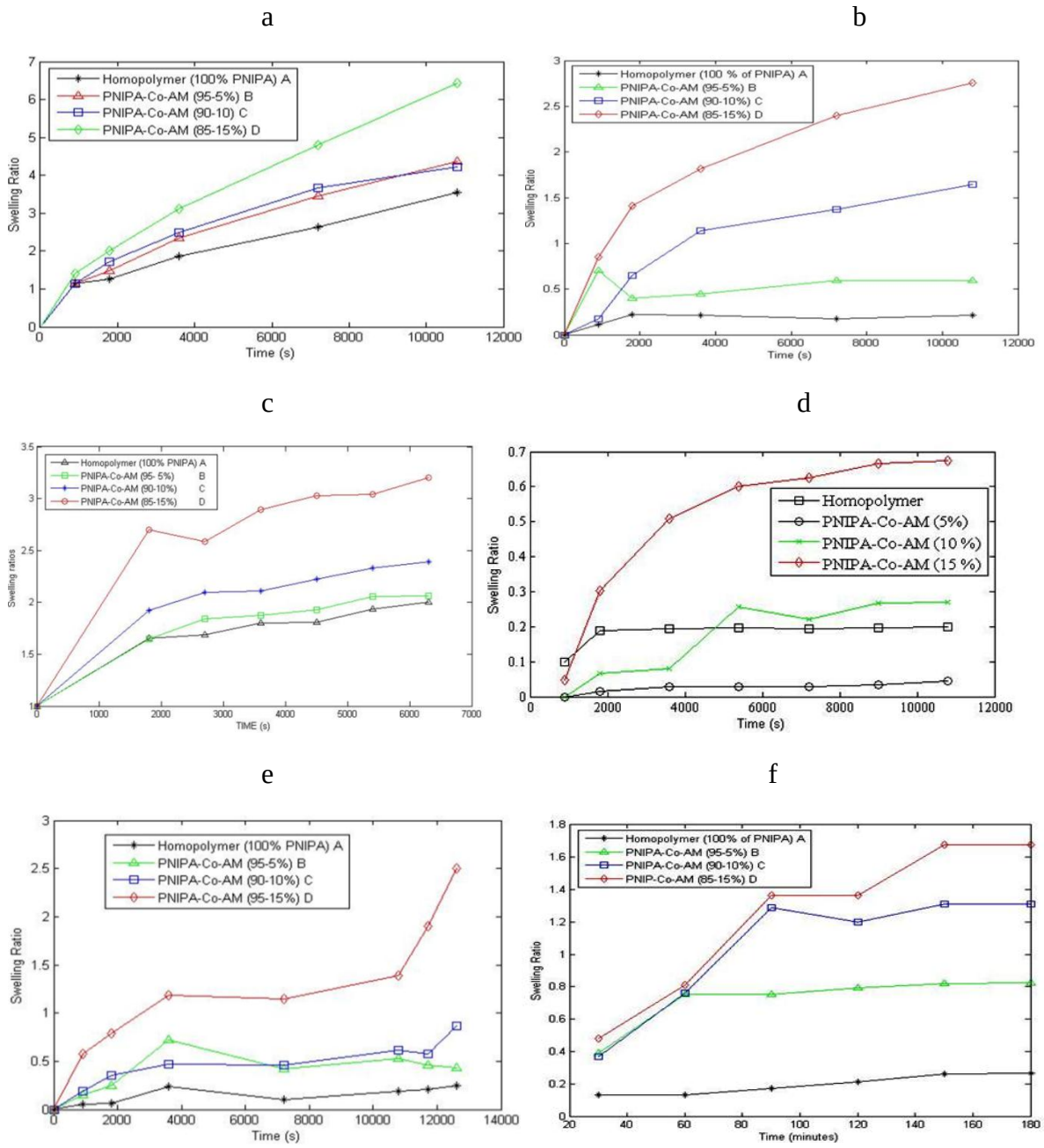

Figure 4.11 Plot of Swelling Ratio of PNIPA-based gels in Bromophenol Blue Verses Time (s): (A) at 28˚C; (B) at 37˚C; (C) at 41˚C; (D) at 43˚C; (E) at 45˚C, and at 48˚C.

It is clear from the above results that the swelling ratios increased with increasing acrylamide content (Figures 4.11a, b, c, e, and f and Tables A and B). In the case of the prodigiosin, the plots of swelling ratio versus time are presented for temperatures between 28 and 48˚C in

Figures 4.12a-f, respectively. Furthermore, the swelling ratios decreased with increasing temperature as shown in Figures 4.12a-b.

A B

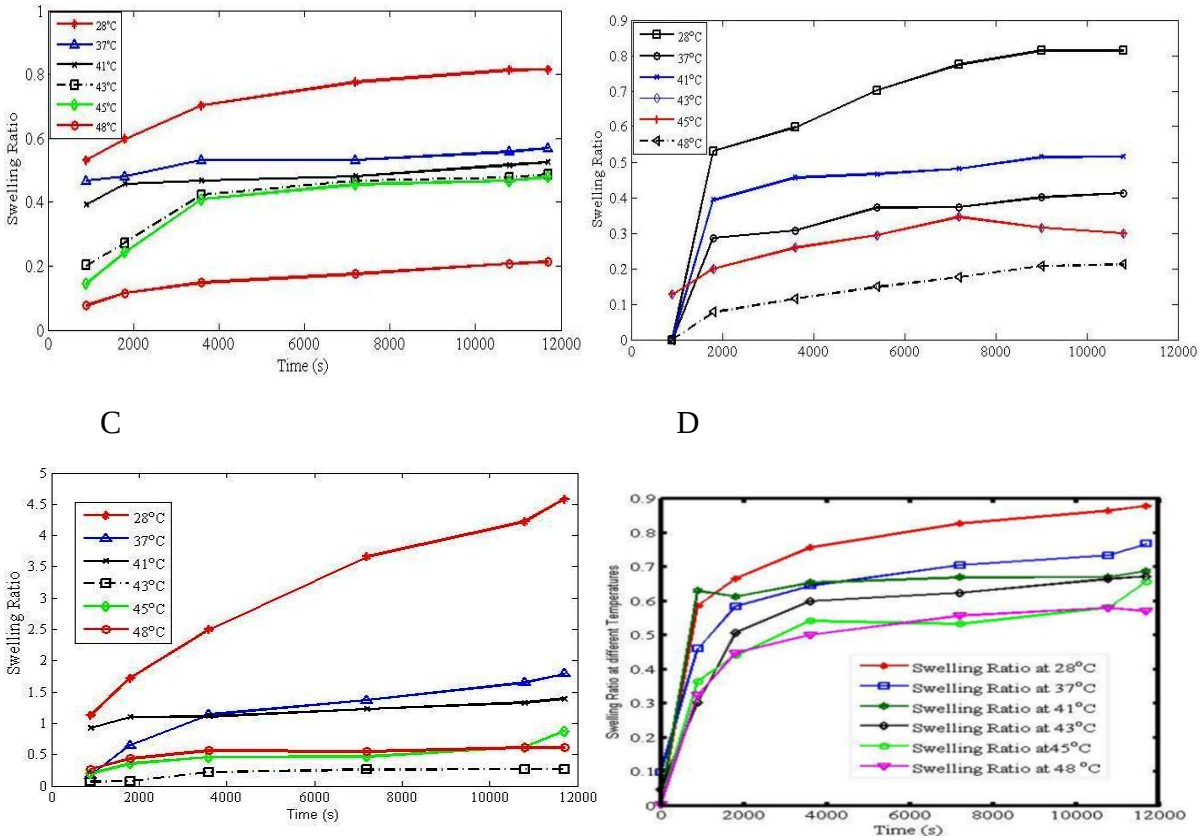

C D

Figure 4.12 Plot of swelling ratio of gels; (a) gel A at different temperatures; (b) gel B at different temperatures; (c) gel B at different temperatures, and (d) gel D at different temperatures.

The diffusion processes of bromophenol blue and or prodigiosin were sensitive to temperature. Plots of swelling ratio at different temperatures are given (Figure 3.12a-d). Similar trends were observed for swelling in water, dye and prodigiosin. However, the magnitudes of the swelling ratios were different in the three environments (Figures 4.13a-d). The diffusion continuous until it plateau when diffusion is at equilibrium after several hours of say (12 hours).

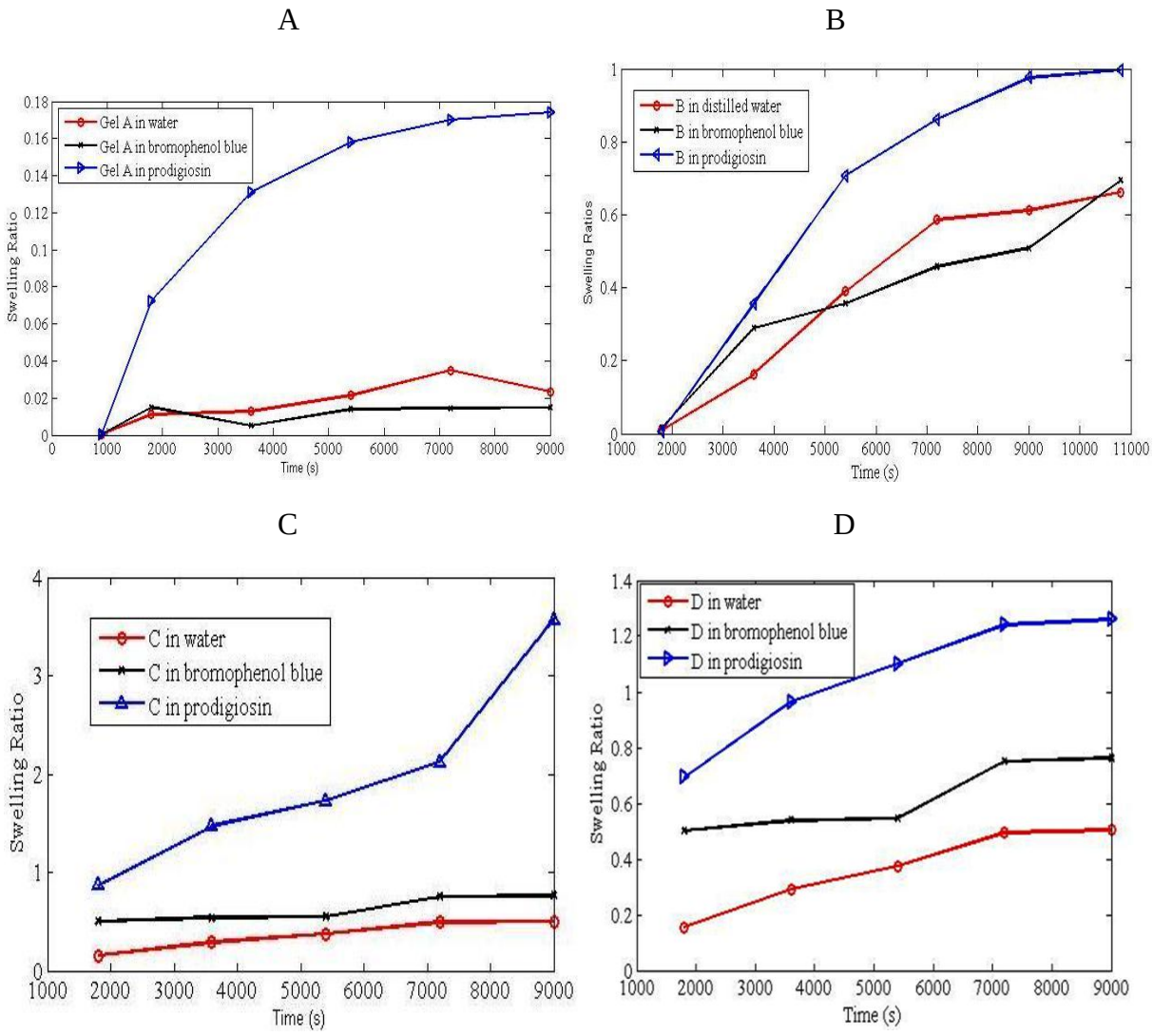

Figure 4.13 Swelling ratios soaked in distilled water, prodigiosin, and bromophenol blue; (a) homopolymer; (b) gel B; (c) gel C, and (d) gel D.

The swelling ratios of the three fluids (i.e water, prodigiosin, and bromophenol blue) were distinguished by the following graphs (Figures 4.13a-d). The absorption of prodigiosin revealed higher values of swelling ratio (Figures 4.13a and b) as compared to water and bromophenol blue. But the swelling of the homopolymer in water was also a little higher than that of bromophenol blue. However, gel B and D absorbed bromophenol blue more than distilled water. It was observed that the swelling ratios of the co-polymers were much greater

in bromophenol blue than when soaked in water which correspond to the increasing amount of hydrophilicity.

4.5 Fluid or Drug Release from PNIPA-Based Gels

The fluid or drug release data obtained for the different gels are presented in Figures 4.14a-d for release from gels A-D at 37˚C. The plots (Figure 4.14a-d) shows the number of moles of fluids absorbed per grams of polymer. These show that, higher moles of prodigiosin per polymer were released. A comparism was made in Figure 4.15 which shows the copolymers absorbs more fluids than the homopolymer.

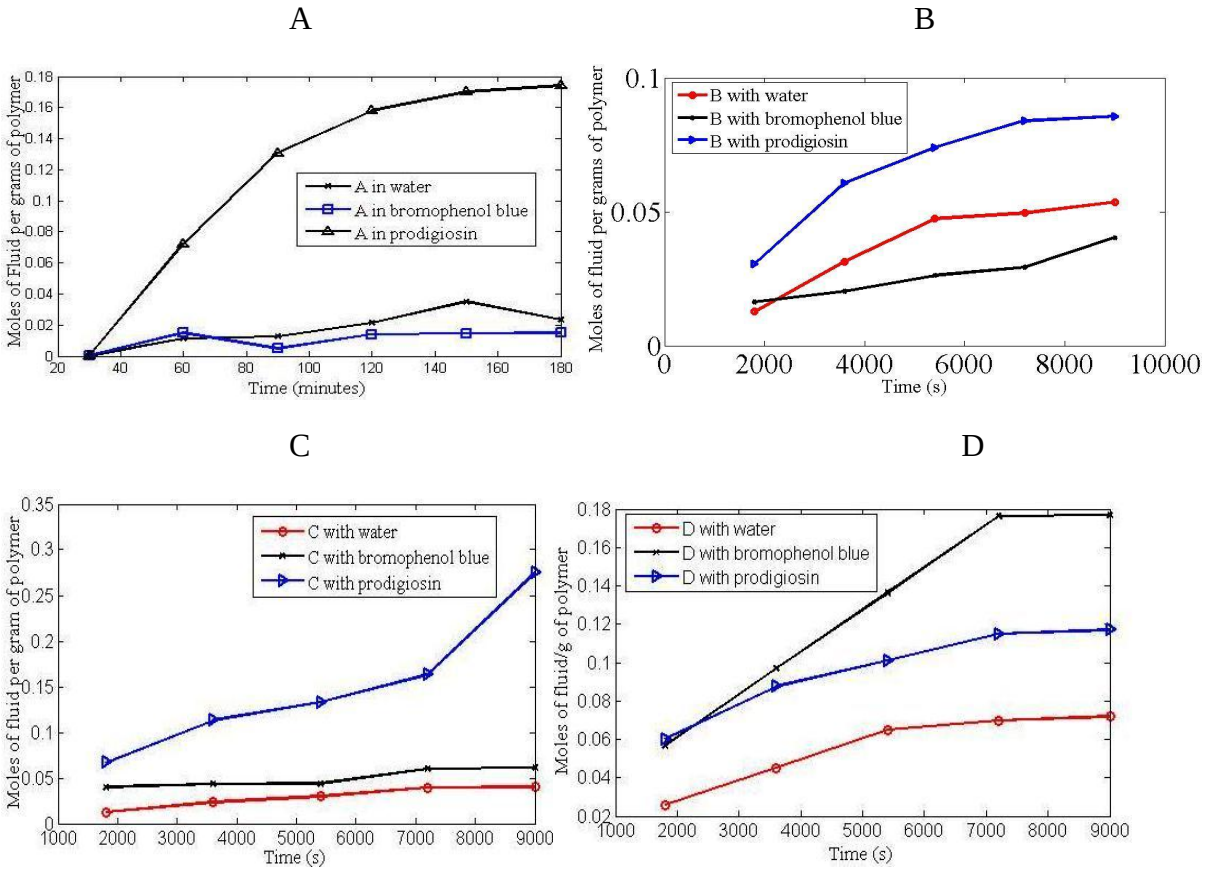

Figure 4.14 Release Profiles of three fluids with gels at 37oC: (a) Homopolymer; (b) PNIPA-Co-AM (5%); (c) PNIPA-Co-AM (10%), and PNIPA-Co-AM (15%).

It was noted that the absorption capacity of the fluids by the co-opolymers tends to increase with the concentration of acrylamide in the PNIPA. Meanwhile the absorption of prodigiosin thus reduces and become less in the released experiment by the gels.

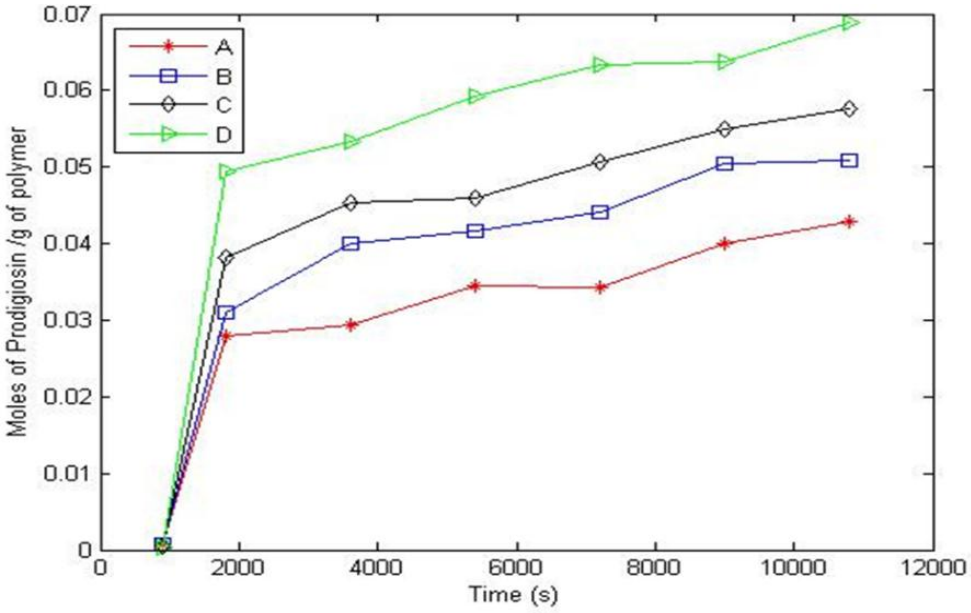

Figure 4.15 Moles of prodigiosin per grams of polymer versus time (s) with PNIPA-based gels at 37oC.

4.5 De-Swelling Ratios

The results obtained from the de-swelling experiments are presented in Figures 4.16a-f for temperatures between 28 and 48˚C. The results show that the de-swelling was temperature dependent. Thus de-swelling was improved by higher temperatures. Thus, the diffusion process was controlled by temperatures. Moreover, copolymers released more fluid than the homopolymers.

A B

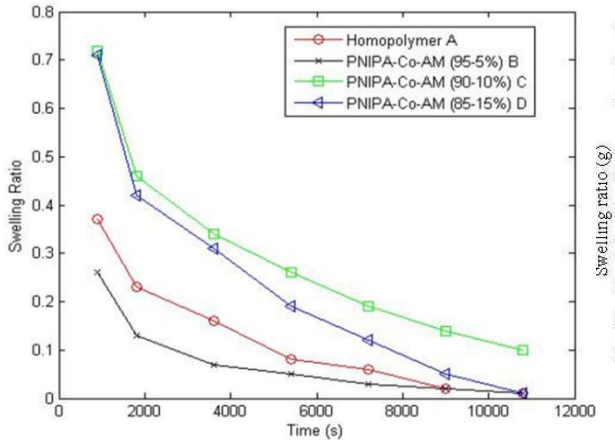

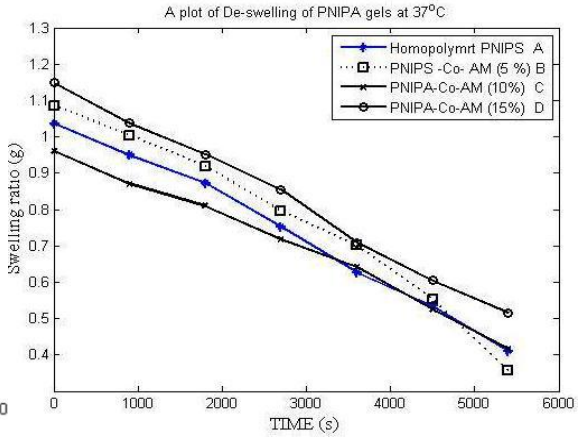

C D

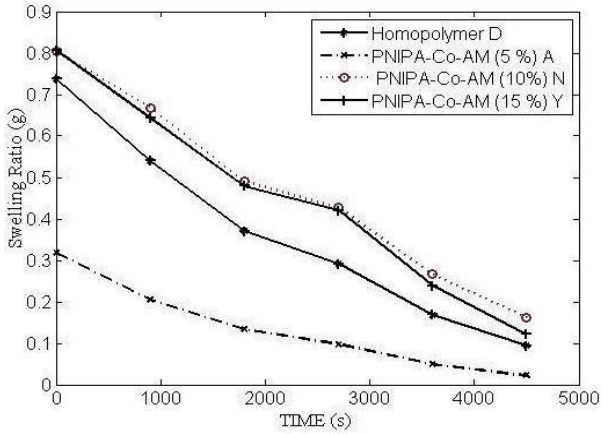

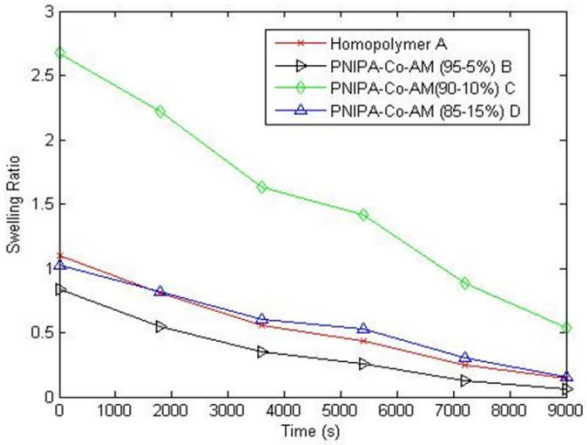

E F

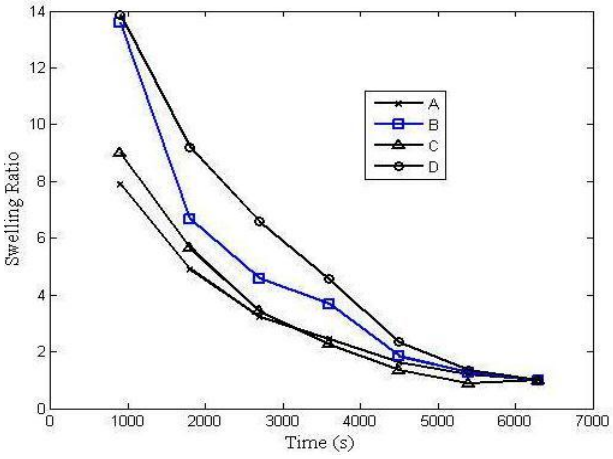

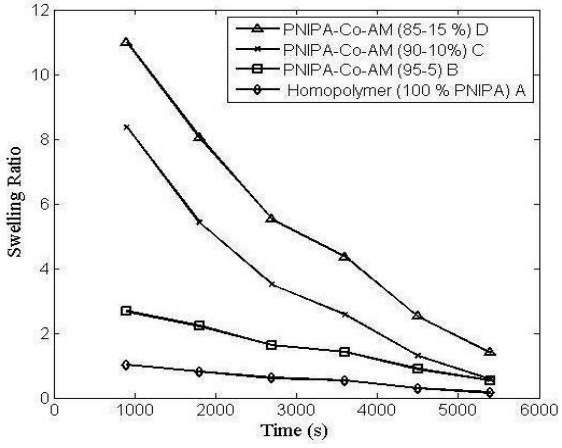

Figure 4.16 Plot of de-swelling ratio of PNIPA and co-polymers of PNIPA from bromophenol blue; (a) at 28˚C; (b) at 37˚C; (c) at 41˚C; (d) at 43˚C; (e) at 45˚C, and (f) at 48 ˚C.

4.6 Release of Fluids from PNIPA-base Gels

The fluid release kinetics from the gels were determined after soaking the dried PNIPA-base gels in water, bromophenol blue, and prodigiosin. The released profiles of fluids from the gels is presented in Figures 4.17. The fluid release rates were generally faster in gels that contained higher acrylamide contents. However, at low acrylamide contents, the release rates in the homopolymer were comparable to those in the copolymers. Similar trends were observed in the release kinetics for water (Figure 4.17a), dye (Figure 4.17b) and prodigiosin (Figure 4.17c).

However, the magnitudes of the release were different. Furthermore, all the gels released $\sim 90\,\%$ of the bromophenol dye and the prodigiosin in ~ 150 minutes at 37˚C. The fluid release rates were also dependent on temperature, as shown in Figure 4.18.

A B

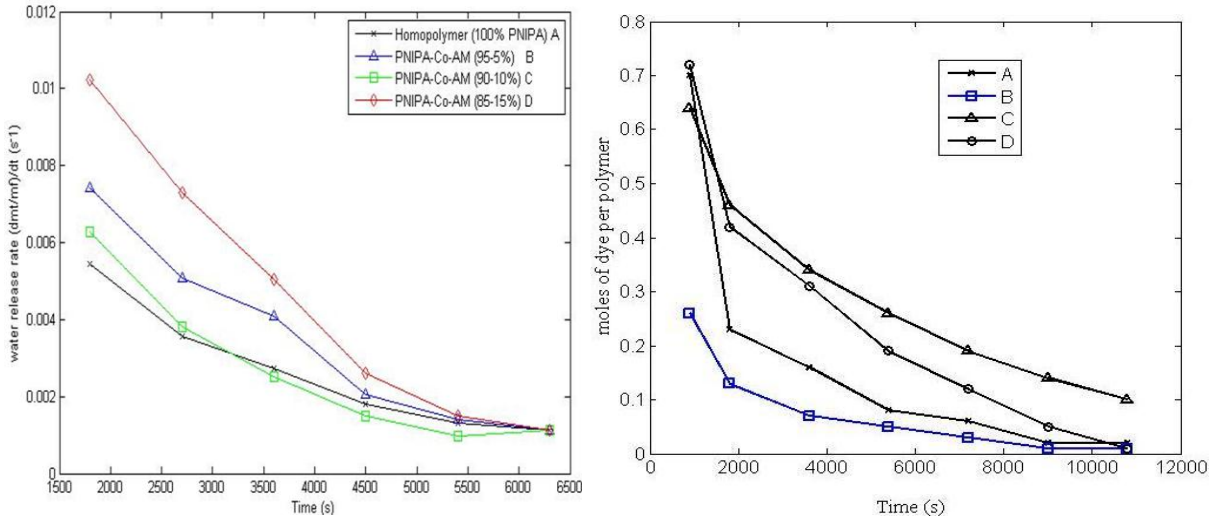

1Figure 4.17 plot of fluid release released rated of PNIPA gels at 43˚C: (a) water and (b) bromophenol blue.

C

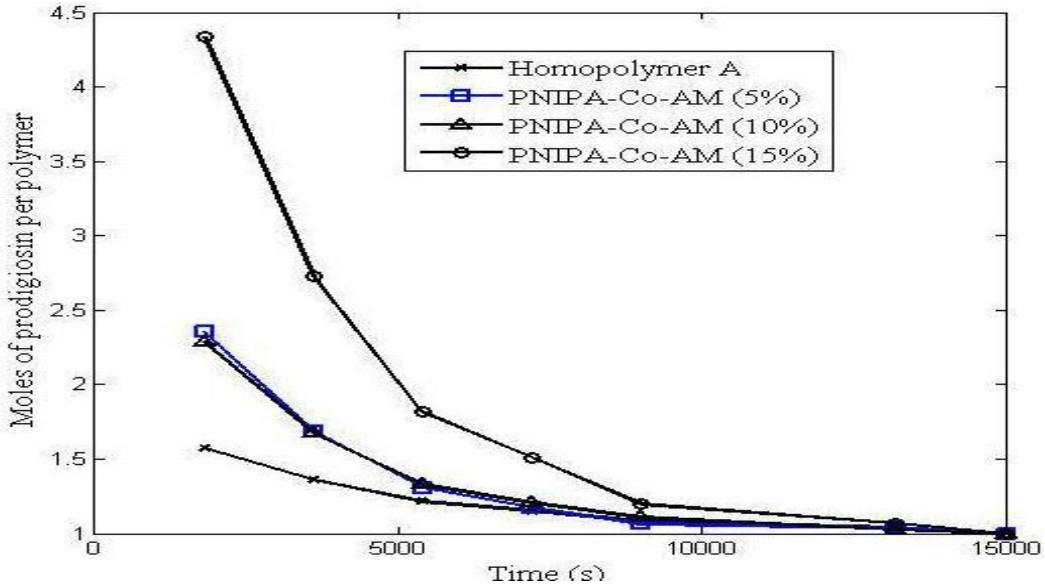

Figure 4.17 plot of fluid release released rated of PNIPA gels at 43˚C; (c) prodigiosin.

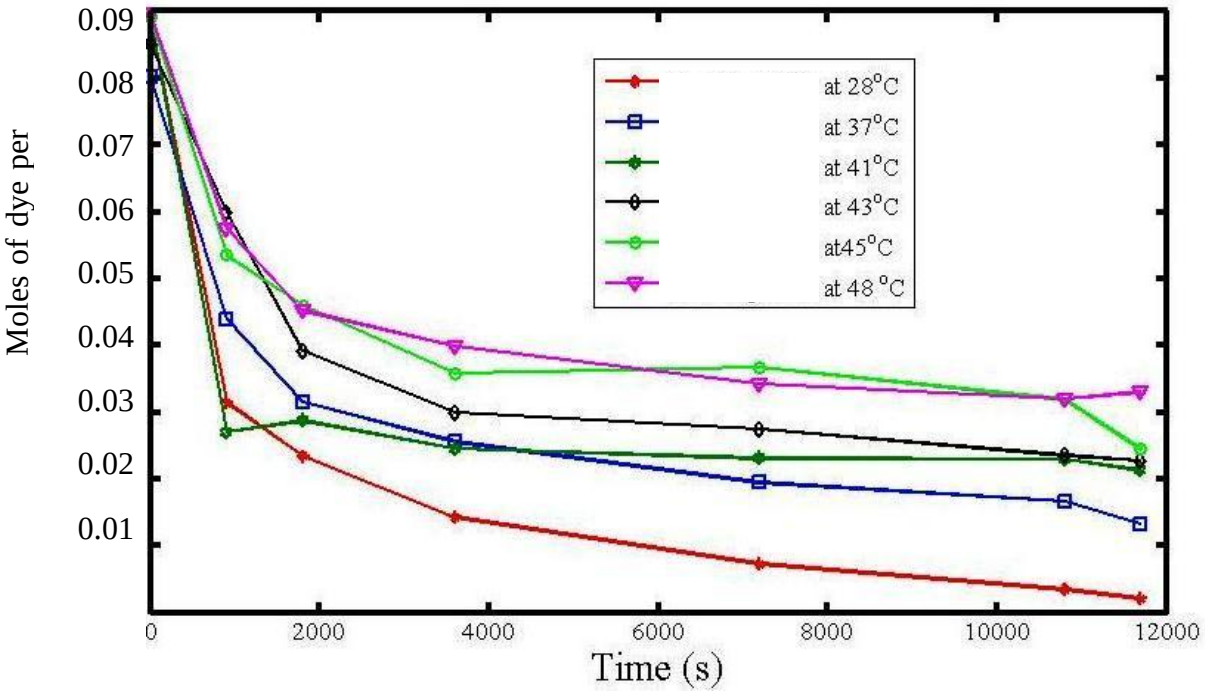

Figure 4.18 plot of dye release released from PNIPA gels at 43˚C

4.7 Mechanism of Drug Release

Efforts have been made over some time which helped to understand the release mechanism of hydrogels (Peppas, 1985), (Siepmann and Peppas, 2001; Hedeenqvist et al., 1996). Based on this prior knowledge, the release of solutes is governed by both the diffusion and viscoelastic behavior of the swollen gels. The released exponent (n) and the dependent constant via diffusion system (k) were determined as given in equation (4.4) (Siepmanna and Peppas, 2000):

$$\frac{m_t}{m_\infty} = 4\left(\frac{Dt}{\delta^2}\right)^n = kt^n \tag{4.4}$$

where $\frac{m_t}{m_\infty}$ is the drug release fraction at time t, k is the constant relating the structural and geometric characteristics of the controlled release, and n is the release exponent which indicates the mechanism of drug release. Equation (4.4) was further used to describe the Fickian diffusion and viscoelastic swelling of the hydrogels. A logarithm equation was deduced from equation to obtain the release of bromophenol blue and prodigiosin by each gel (A-D).

$$\ln\left(\frac{m_t}{m_\infty}\right) = \ln + n\ln t \tag{4.5}$$

The linear plots of $\ln\left(\frac{m_t}{m_\infty}\right)$ versus $\ln t$ are presented in Figure 4.19. The values of n, k and their corresponding R^2 are given in Table 4.3. The diffusion coefficient D was obtained by:

$$D = \frac{k\pi\delta^2}{4} \tag{4.6}$$

where $\delta\ is$ the thickness of the hydrogel (~0.003m) and k is the intercept from the graph relating to what is known as the geometry constant.

Table 4.3 Summary of n, k and R^2 values for the various gel composites at 28˚C in bromophenol blue.

Gel Code	Release exponent (n)	The geometric/ structural constant (k)	$Regression\ coefficient\ R^2$
A	0.49	0.97	0.94
B	0.54	0.89	0.92
C	0.60	0.87	0.93
D	0.67	0.75	0.85

The data for the release of bromophenol blue through the gels was fitted linearly to equation 4.5. Gel A was found to have a release exponent of 0.49, i.e equal to 0.5. This is consistent with Fickian diffusion in gel A. Hence, the release rate would proportional to $t^{-0.5}$. The released exponents of the other gels varied between 0.54 – 0.67. This is anomalous, since n is greater than 0.5 (Peppas, 1985). Hence the drug transport mechanism is by a non-Fickian diffusion mechanism. It is also important to note that the release exponent increased with increasing amount of acrylamide (hydrophilic compound), while the geometric factor, K, decreases with increasing acrylamide content.

The Plots of $\ln\left(\frac{m_t}{m_\infty}\right)$ versus $\ln t$ for the various gels are presented for different temperatures between 28 and 48˚C in Figures 4.19a-f. Figure 3.15a-f, while the corresponding values of n, k and their corresponding r^2 values are summarized in Table 4.4-4.8.

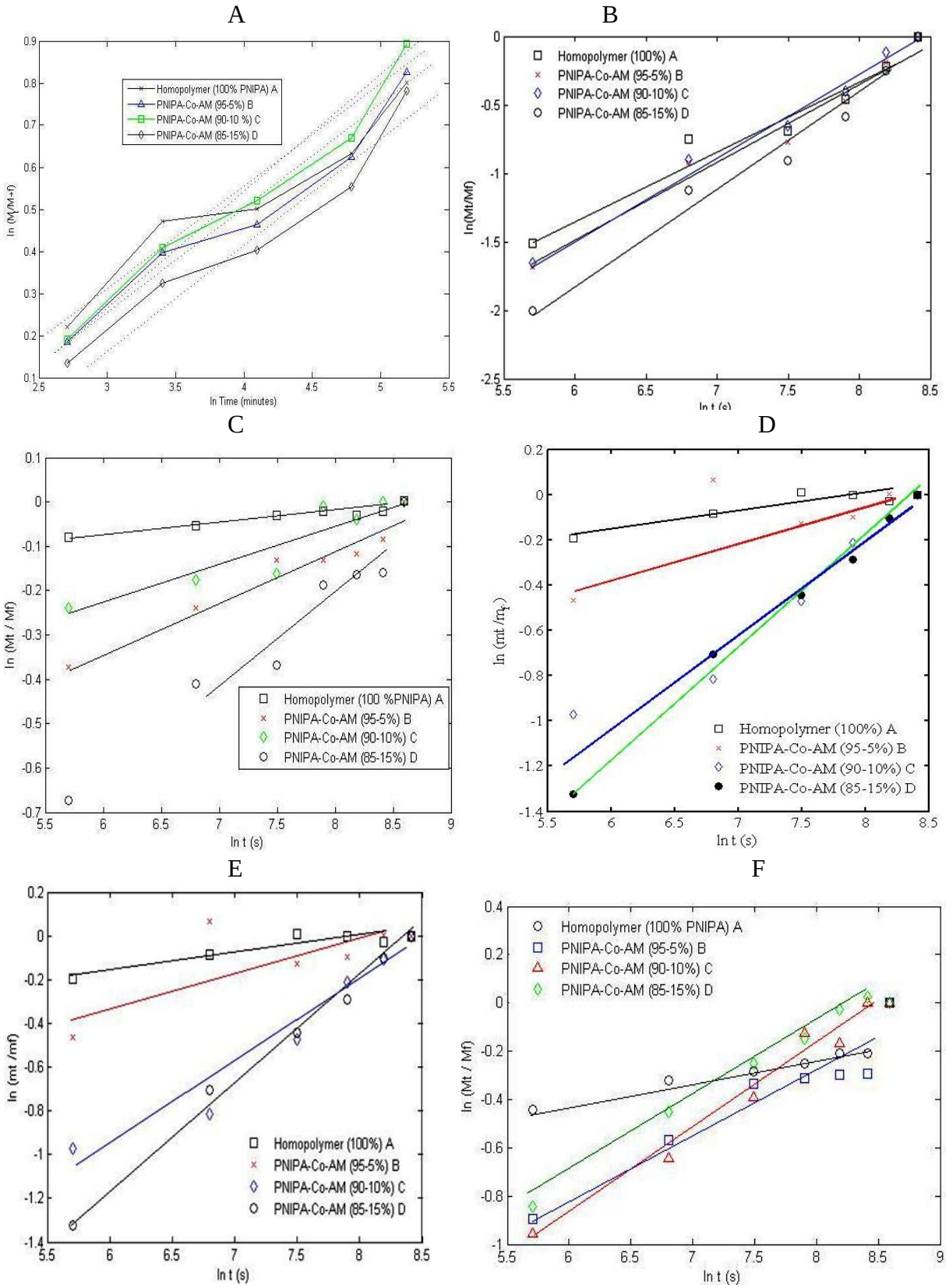

Figure 4.19 Diffusion fit for bromophenol blue, plot of ln⁡〖M_t/M_∞ 〗 versus In t (s) for PNIPA gels hydrogels: (a) at 28˚C; at 37˚C; (d) at 41˚C; (d) at 43˚C; (e) at 45˚C and (f) at 48˚C.

Table 4Table 4.4 Summary of n, k and R^2 values for the various gel composites of prodigiosin at 37˚C.

Gel Code	Release exponent (n)	The geometric/ structural constant (k)	R^2	Diffusion Coefficient, D (m^2/s)
A	0.5	0.01	0.95	3.56E-09
B	0.6	0.01	0.97	9.66E-10
C	0.6	0.01	0.99	9.65E-10
D	0.7	0.01	0.97	1.42E-10

The table above depicts that acrylamide which is a hydrophilic compound tends to be water loving and, hence overall diffusion rate is lower; gel D was lower for lower temperatures but increases with temperatures. The value of n is dependent on the amount of the ionic groups in the hydrogel. The value of the release exponent therefore seems to increases largely with increasing acrylamide content. The exponential outcome indicates that when the crosslinker ratio of (AM/MBA) increases, it causes the n exponent to rise which causes the value of k to decrease.

Table 4.5 Summary of n, k and R2 values for the various gel composites at 43˚C.

Gel Code	Release exponent (n)	The geometric/ structural constant (k)	R^2	Diffusion Coefficient, D (g/s)
A	0.17	0.68	0.90	4.81E-06
B	0.80	0.17	0.95	1.21E-06
C	0.63	0.26	0.85	1.80E-06
D	1.4818	0.0378	0.9431	2.6863E-07

The release exponent for all the gels respectively indicated an anomalous mechanism, and thus superposition of diffusion and de-swelling (Oni, 2011).

Table 4.6 Summary of n, k and R2 values for the various gel composites 45˚C.

gel code	Release exponent (n)	The geometric constant (k)	Regression coefficientR^2	Diffusion Coefficient, D (g/s)
A	0.45	0.35	0.86	2.49E-06
B	0.98	0.13	0.56	9.00E-07
C	0.48	0.02	0.99	1.27E-07
D	0.38	0.04	0.94	2.78E-07

Table 4.7 Summary of n, k and r2 values for the various gel composites 48˚C.

gel code	Release exponent (n)	The geometric constant (k)	Regression coefficient, R^2	Diffusion Coefficient, D (g/s)
A	0.81	0.15	0.75	1.08E-06
B	0.26	0.10	0.91	6.76E-07
C	0.35	0.05	0.98	3.69E-07
D	0.30	0.08	0.99	5.55E-07

4.8 Modeling of Fluids/ Prodigiosin Release

The loaded gels were released at setting temperatures (28˚C-48˚C) whiles the released diffusivity through the polymer network was modeled with the early time approximation (equation 4.7a), and that of the late time approximation (equation 4.7b) (Heller et al, 2004; Baker et al, 1974).

$$\frac{dM_t}{dt} = 2M_{total}\left(\frac{D}{\pi\delta^2 t}\right)^{1/2} \qquad (4.7a)$$

$$\frac{dM_t}{dt} = \frac{8M_{total}}{\delta^2}\left(\frac{-D\pi^2 t}{\delta^2}\right)^{1/2} \qquad (4.7b)$$

where $\frac{dM_t}{dt}$ corresponded to the fluid released rate, M_t is the amount of fluid released at time t, M_{total} is the total amount of substance that was dissolved in the PNIPA hydrogels, D is the diffusion coefficient, and δ is the thickness of the dried hydrogel (Figure 4.20)

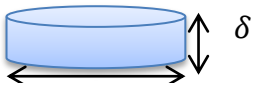

Diameter

Figure 4.20 illustration of gel

Equation (4.7a) was solved to obtain its linear form as:

$$\frac{d\left(M_t/M_{total}\right)}{dt} = \frac{2D^{\frac{1}{2}}}{\pi\delta^2} * (t)^{-\frac{1}{2}} = A * (t)^{-\frac{1}{2}} \qquad (4.7c)$$

Where the coefficient $= \frac{2D^{\frac{1}{2}}}{\pi\delta^2}$.

The release rate was best described by a linear equation of the form: $\frac{d\left(M_t/M_{total}\right)}{dt} = A(t)^{-\frac{1}{2}}$ where A- corresponds to the gradient from the linear graph (Figure 4.20). The release rate was obtained using equation 4.7c as a function of time, t (Figure 4.21). The linear graph of the release rate of prodigiosin shows a rapid increase with time.

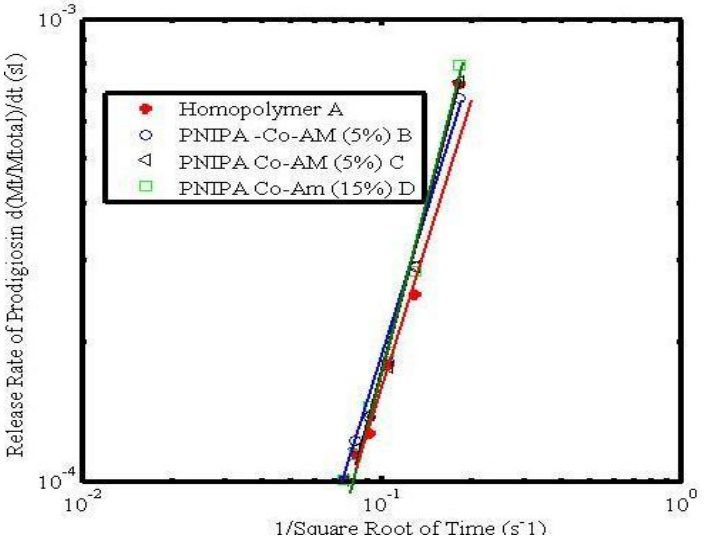

Figure 4.21 Linear plot of the release rate of prodigiosin against time at 41˚C on a log scale.

The release of Bromophenol blue as a function of time is given (Figure 4.22a-b).

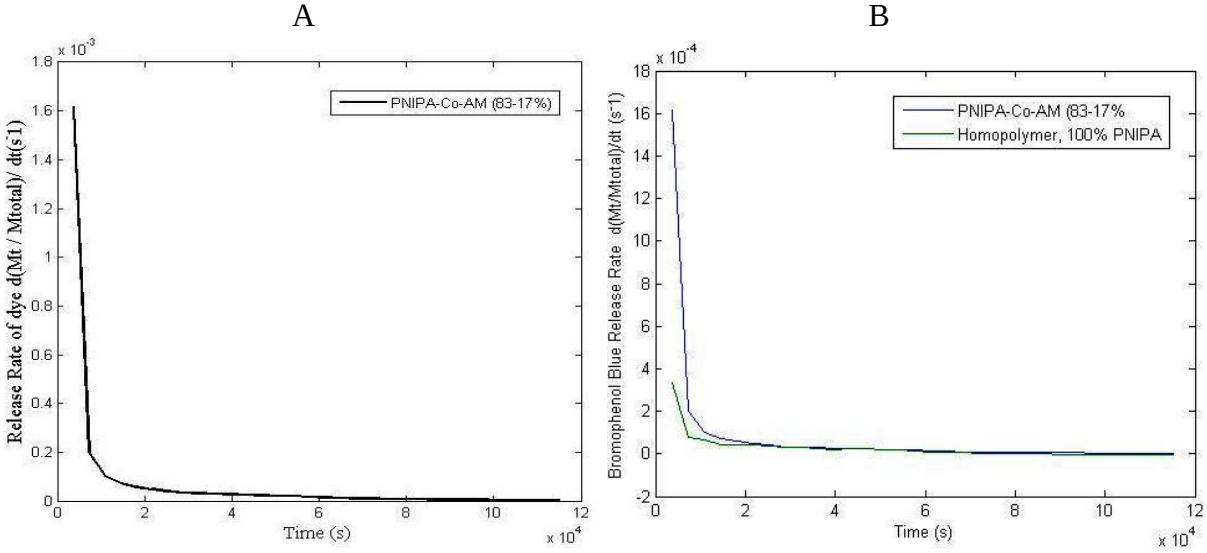

Figure 4.22 Release Rates of bromophenol blue at 28˚C: (a) Hydrophilic Co-polymer (17% acrylamide); (b) Hydrophilic Co-polymer (17% acrylamide) and a homopolymer.

The release rate is higher at the earlier time scales when the release commenced because of the full saturation of the fluid at the interface of the gel which requires no or less pressure to flow out. However, the release rate decreases due to lower pressure within the gel network to squeeze out the dye/drugs.

The release rates were higher for the hydrophilic PNIPA co-polymers as compared to the PNIPA homopolymer. The graph is figure 3.18b above revealed the lower released profile of the homopolymer when compared to the gel with 17 % acrylamide. This is due to the fact that, the acrylamide which is a hydrophilic compound creates micro-porous network as illustrated from the SEM analysis. This microporous network encourages more fluids to be entrapped in the gel.

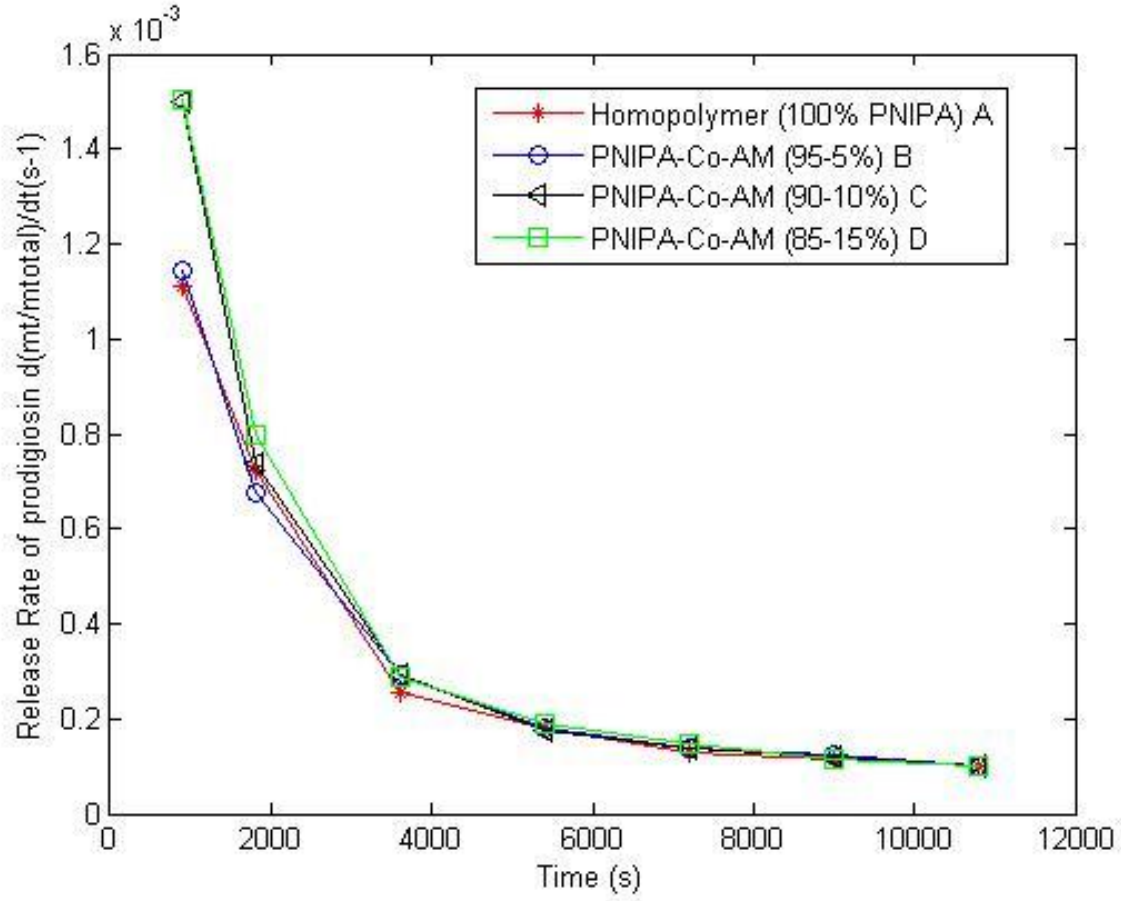

Figure 4.23 Release Rate of Prodigiosin at 41˚C through PNIPA and hydrophilic co-polymers.

The initial release rates were rapid and subsequently degraded with time. This was as a result of saturated fluid on the surface of the gel prior to swelling. The reduction in release profile could be best explained by a reduction in fluid content in the gel and also a reduction in pressure to induce flow of fluid from the gel network. Hence, this lowered the release rate.

The absorption of prodigiosin as shown in the figure above was due to the hydrophilic nature of the polymer network. The addition of acrylamide to PNIPA increases the absorption capacity of prodigiosin. The amount of prodigiosin absorbed per grams of polymer is indirectly correlated to the amount of acrylamide. Increasing the acrylamide content in the gel will encourage the absorption of fluids such as prodigiosin, bromophenol blue, and water.

The diffusion coefficients of the gels are summarized in Table 4.8 and 4.9. The activation energy for each gel was obtained from a plot of diffusion coefficient as a function of temperature using the Arrhenius form of equation (Figures 4.24a-d) for gel A-D:

$$D = D_o exp\left(\frac{-E_a}{RT}\right) \quad (4.8)$$

Where R is the Gas constant, T is temperature; E_a is the activation energy for each gel. The activation energies for the gels are presented in table 4.10. When equation (4.8) was linearized, a straight line graph was obtained by plotting the diffusion.

Table 4.8 summarized the diffusion coefficients at different temperatures for PNIPA and PNIPA co-polymers.

Gel Code	Temperatures in degrees Celsius (˚C)					
	28	37	41	43	45	48
	Diffusion coefficients (m^2/s) for PNIPA and hydrophilic PNIPA					
A	$2.28x10^{-11}$	$1.072x10^{-10}$	$1.87x10^{-9}$	$1.02x10^{-9}$	$4.18x10^{-8}$	$5.60x10^{-9}$
B	$2.10x10^{-12}$	$2.54x10^{-10}$	$1.38x10^{-11}$	$1.59x10^{-11}$	$4.40x10^{-11}$	$1.38x10^{-11}$
C	$1.59x10^{-11}$	$1.02x10^{-9}$	$2.11x10^{-8}$	$5.62x10^{-9}$	$1.90x10^{-9}$	$2.80x10^{-9}$
D	$2.38x10^{-10}$	$1.02x10^{-9}$	$2.11x10^{-8}$	$5.622x10^{-9}$	$1.90x10^{-9}$	$2.80x10^{-9}$

Table 4.9 Diffusion coefficients for the hydrogels were compared at 35˚C in three fluids

Gel Code	Diffusion coefficient in distilled Water (m^2/s)	Diffusion coefficient (m^2/s) in Bromophenol blue	Diffusion coefficient (m^2/s) in Prodigiosin
A	1.56×10^{-9}	8.07×10^{-10}	2.45×10^{-10}
B	4.65×10^{-9}	1.14×10^{-8}	5.09×10^{-8}
C	7.86×10^{-9}	4.51×10^{-10}	1.76×10^{-10}
D	1.41×10^{-8}	1.24×10^{-9}	1.50×10^{-9}

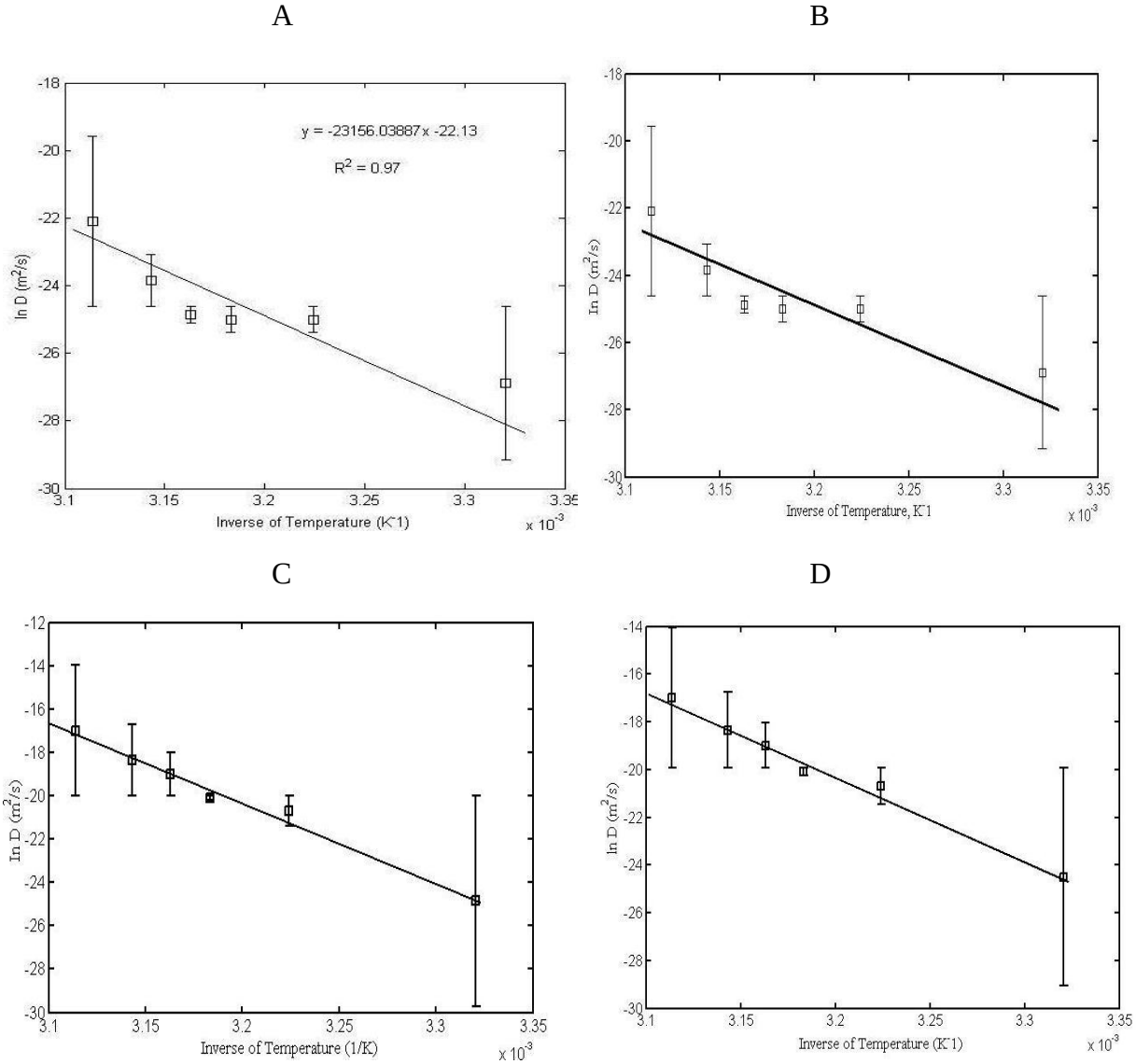

Figure 4.24 Plots of ln D versus 1/T (K-1): (a) for gel A; (b) for gel B; (c) for gel c, (d) and for gel D.

Table 4.10 Activation energy of the gels

Gel Code	Activation Energy (KJ/mole)
A	190.905
B	192.542
C	207.390
D	224.251

4.9 Surface Texture of PDMS for better integration into the body

Various textured surfaces were obtained on the micro scale with a mold on the BioMEMS. Three types of surface textured have been proposed for the BioMEMS as shown below (Figure 4.25a-c). These surfaces will enhance cell migration especially if proteins such as RGD peptides are grown on the surface of the device before implanting to enhance the device to be well integrated into the body.

A 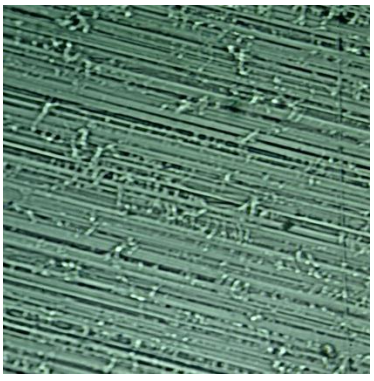 B 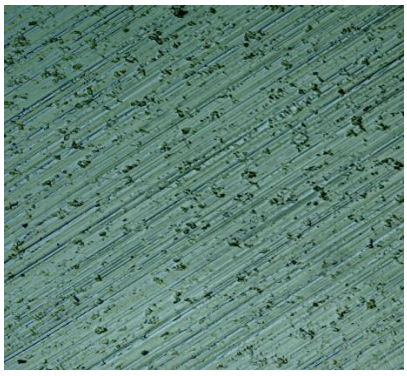 C 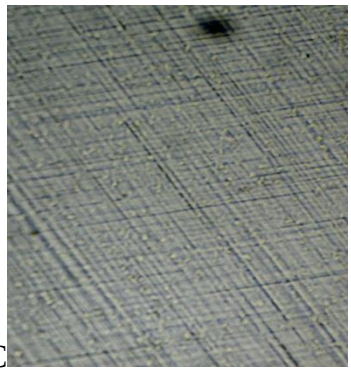

Figure 4.25(a-c) shows the textured surfaces of the PDMS obtained with an aluminum mold

4.10 Discussion

The typical behavior of PNIPA gel is their temperature responsive and their ability to exhibit a volume phase transition. The process in gelation changes from a homogeneous to heterogeneous. This helps in fast response with the hydrogels. PNIPA gels will then shrink at temperatures above their transition temperature. The macro-porous network enables PNIPA to soak in fluids/ water. The adsorption/ desorption of water/ fluid therefore occurs through the interconnected pore structures by convection (Yual and Oguz, 2005).

The macro-porosity of PNIPA gel depends on factors including; the phase separation during crosslinking, the gel synthesis parameters such as the preparation temperature, crosslinkers, monomer concentration, and then the pore-forming agent used. But among all these parameters, the gel preparation temperature matters most since it has a great influence on the macro-porosity within the PNIPA gel network. As a matter of fact, it implies that polymerization below the lower critical solution temperature (LCST) would help achieve the macroporous gel network.

The release rates of fluids from PNIPA gels followed the early time approximation equation (Heller et al., 2004) which fits $a\ curve\ of\ t^{-\frac{1}{2}}$. The release rate was best described by a linear equation by the form: $\frac{d\left({}^{M_t}/_{M_{total}}\right)}{dt} = A(t)^{-\frac{1}{2}}$. The rate of elution of bromophenol blue, prodigiosin, and water was observed to decrease rapidly within the earlier hours, falling as a function of $t^{-\frac{1}{2}}$, and subsequently, the release rate exponentially decayed. The reduction in elution caused the PNIPA hydrogel to collapse in its dried state especially when the fluid is completely discharged from it.

The diffusion coefficients obtained varied from 2.10 x10^{-12} m^2/s at 28˚C to 4.8162x10^{-6} m^2/s at

48˚C. The rate of diffusion was fueled by higher temperatures. Also, the diffusion coefficients for the co-polymers were averagely greater than those obtained for the homopolymer which can be due to the presence of macro-porous gel network as results of acrylamide (hydrophilic compound). The diffusion coefficient was higher in the hydrophilic PNIPA which yielded a diffusion coefficient of $1.13x10^{-12}$ m^2/s to $4.18\ x10^{-8}$ m^2/s.

The results obtained from the released exponent as well as the diffusion coefficient from the gels were consistent to prior work (Oni et al., 2011; Matsuo and Tanaka, 1994). The work from Matsue et al., 1994, indicated diffusion coefficients of PNIPA which were found to be within $0.2\ x\ 10^{-12}$ m^2/s and $4\ x\ 10^{-12}$ m^2/s., which was said to be dependent on the network densities of the gels. The work from Oni et al, 2011 also revealed diffusion coefficient of PNIPA within $1.68x10^{-12}$ m^2/s at 37˚C to $1.12x10^{-6}$ m^2/s at 45˚C.

The modeled results were fitted to the release profiles with prodigiosin and bromophenol blue at temperatures of 37˚C, 41˚C, and 43˚C. This was done to simulate body temperature; hence hyperthermia could be effective at temperatures above 37˚C. The monolithic diffusion model described the diffusion of prodigiosin and bromophenol blue from the PNIPA and PNIPA co-polymers. The diffusion coefficients of gels soaked with prodigiosin, bromophenol blue, and water is summarized in Table 3. Despite the numerous advantages of hydrogels, they suffer the challenge of poor mechanical properties especially during their swollen stages.

4.11Reference for chapter four

- Baker R.W., Lonsdale H.K. in: Tanquary A.C. and Lacey R.E (1974), "Controlled Release of Biologically active Agents", Plenum Publishers, New York, pp. 15-71.
- Heller J. and Hoffman A. S., Ratner in B D, Ho man A. S., Schoen F. J., Lemonsm J. .E (Ed) (2004), "Biomaterials Science". Academic Press, New York, pp629-630.
- Kaneko, Y.; Sakai, K.; Kikuchi, A.; Yoshida, R.; Sakurai, Y.; Okano, T (1995). Macromolecules, 28, 7717.
- Matsuo E.S., Tanaka T., Phase Transitions, 46 (1994) 217.
- Oni C. Theriault, Hoek A.V., Soboyejo W.O. (2011), "Effects of temperature on diffusion from PNIPA-based gels in a BioMEMS device for localized chemotherapy and hyperthermia", Materials Science and Engineering C, pp67-76.
- Tanaka T. (1981) Gels. Sci. Am. 244 124.
- Yoshida, R.; Uchida, K.; Kaneko, Y.; Sakai, K.; Kikuchi, A.; Sakurai, Y.; Okano, T. Nature 1995, 374, 240.
- Yual Dogu, Oguz Okay (2005), "Swelling–Deswelling Kinetics of Poly(Nisopropylacrylamide) Hydrogels Formed in PEG Solutions", Wiley InterScienceInc. Journal of Applied Polymer Science 99: pp37–44.

5.0 CHAPTER FIVE

5.1 Implications of the Results

The fast response rate of PNIPA to an external stimulus draws much attention toward their application in drug delivery. The rate of swelling or shrinking of PNIPA gels is usually controlled by the diffusion of water molecules through the gel network. Though this process may be slow especially near the critical point, yet the rate of response is inversely proportion to the square of the gel thickness. The studies have shown dangling chains structure of PNIPA gels which agreed with prior works (Yoshida, 1995), (Kaneko, 1996). This implies a gel would easily collapse and expand when an external stimulus is applied, as a result of the free dangling chain on the side.

The values for the release exponent, n were mostly dependent on the amount of the ionic groups in the hydrogel. The exponential outcome also indicated that increasing the crosslinker ratio of methylene-bisacrylamide and acrylamide would sometimes cause the release exponent (n) to rise.

The BioMEMS delivering system is made of a PNIPA gel encapsulated into a reservoir in the PDMS gel which is a polymer membrane. The elucidated fluids from the prototype device within the laboratory environment occurred by diffusion across the membranes. The PDMS was observed under the optical microscopy and SEM to be nonporous.

The diffusion through the micro-channel can be represented by Fick's law.

$$J = -D\left(\frac{dC_m}{dx}\right) \qquad (5.1)$$

Where J is the flux per unit area (g/cm^2sec), C_m represented the concentration of the drug/bromophenol blue (g/cm^3), D is the coefficient of diffusion (cm^2/sec) of the drug filled in

the PDMS reservoir, and the concentration gradient is represented by $\left(\frac{dC_m}{dx}\right)$. But it is difficult to determine the concentration of the agents in the memebrane.

5.2 Conclusion

This present work presented the diffusion and swelling kinetics of PNIPA gels and its composites at temperatures (28˚C-48˚C). The swelling capacities of the PNIPA gels were found to decrease with temperature given evidence of the thermo-sensitivity of PNIPA gels. The release rates were governed by the earlier time approximation equation and the diffusion of water molecules were under the influence of temperature. Non-Fickian diffusion dominated in all the results obtained with the power law equation (Peppas, 1985).

The biocompatibility of PDMS (Approved by American Food and Drug Association); the macroporous structure of the PNIPA gel; sensitivity PNIPA environmental stimuli such as temperature, calls for a necessary attention toward using PNIPA gels encapsulated with PDMS for localized breast cancer drug delivery.

The drug delivery system can therefore release cancer drugs locally into the tissue surrounding the device. In this way, any remaining cancer cells /tissue can be killed prior to surgery, as the eluted drug flows into the surrounding tissue. Moreover, the synergy of hyperthermia would induce killing of cancer cells surrounding the device. Since the delivery of the drug is localized, the total quantity of drug, that is needed to have a therapeutic effect, may be reduced significantly. Hence, the potential side effects associated with localized cancer drug delivery should be much lower than those associated with bulk systemic chemotherapy.

A local drug candidate – prodigiosin has been considered as a possible cancer drug in this

research. Its release properties have been elucidated along with its sorption pattern into the PNIPA gel. The potentials of this cheaply available drug for cancer chemotherapy is quite enormous.

5.3 Future work

It is recommended that, Differential Scanning Calorimetric Analysis (DSC) could be carried out to determine the lower critical solution temperature of the gels. The future of the multi-modal implant is summarized in the diagram below. We could innovate around the device by incorporating a microprocessor to control the release of drugs from the device, and a radiofrequency identification to monitor the device performance within the body. Moreover, a hyperthermia device as well as a source of power could be incorporated.

The animal studies with the device should be carried out once its performance proves to be favorable in environments that mimic the physiological conditions where the gels would work.

5.4 Reference

- Peppas N. A. (1987), ―Hydrogels in medicine and pharmacy‖, CRC Press, Boca Ratons, FL.

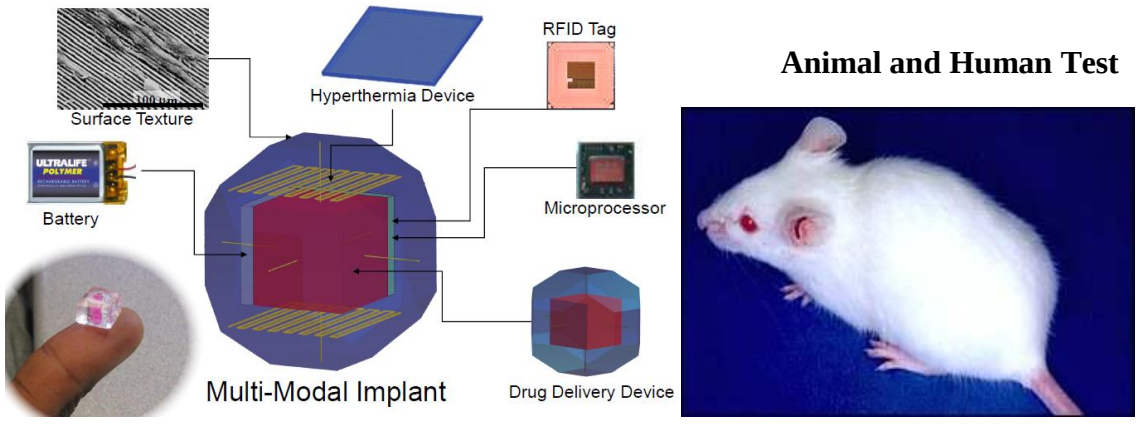

Figure 5.1 The Future Device